Accepted Manuscript

Ring-truncated Deguelin Derivatives as Potent Hypoxia Inducible Factor-1α (HIF-1α) Inhibitors

Ho Shin Kim, Mannkyu Hong, Su-Chan Lee, Ho-Young Lee, Young-Ger Suh, Dong-Chan Oh, Ji Hae Seo, Hoon Choi, Jun Yong Kim, Kyu-Won Kim, Jeong Hun Kim, Joohwan Kim, Young-Myeong Kim, So-Jung Park, Hyun-Ju Park, Jeewoo Lee

PII: S0223-5234(15)30277-4

DOI: 10.1016/j.ejmech.2015.09.033

Reference: EJMECH 8130

To appear in: *European Journal of Medicinal Chemistry*

Received Date: 31 July 2015

Revised Date: 24 September 2015

Accepted Date: 25 September 2015

Please cite this article as: H.S. Kim, M. Hong, S.-C. Lee, H.-Y. Lee, Y.-G. Suh, D.-C. Oh, J.H. Seo, H. Choi, J.Y. Kim, K.-W. Kim, J.H. Kim, J. Kim, Y.-M. Kim, S.-J. Park, H.-J. Park, J. Lee, Ring-truncated Deguelin Derivatives as Potent Hypoxia Inducible Factor-1α (HIF-1α) Inhibitors, *European Journal of Medicinal Chemistry* (2015), doi: 10.1016/j.ejmech.2015.09.033.

Graphical Abstract

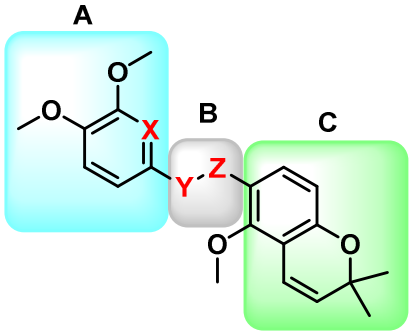

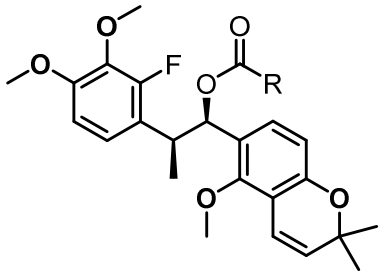

25 R = Me
33 R = Cyclopropyl

Ring-truncated Deguelin Derivatives as Potent Hypoxia Inducible Factor-1α (HIF-1α) Inhibitors

Ho Shin Kim [a], Mannkyu Hong [a], Su-Chan Lee [a], Ho-Young Lee [a], Young-Ger Suh [a], Dong-Chan Oh [b], Ji Hae Seo [c], Hoon Choi [c], Jun Yong Kim [c], Kyu-Won Kim [c,d], Jeong Hun Kim [e], Joohwan Kim [f], Young-Myeong Kim [f], So-Jung Park [g], Hyun-Ju Park [g], and Jeewoo Lee [a,*]

[a] Research Institute of Pharmaceutical Sciences, College of Pharmacy, Seoul National University, Seoul 151-742, Korea

[b] Natural Products Research Institute, College of Pharmacy, Seoul National University, Seoul 151-742, Korea

[c] SNU-Harvard NeuroVascular Protection Research Center, College of Pharmacy, Seoul National University, Seoul 151-742, Korea

[d] Department of Molecular Medicine and Biopharmaceutical Sciences, Graduate School of Convergence Science and Technology, Seoul National University, Seoul 151-742, Korea

[e] College of Medicine, Seoul National University, Seoul 151-742, Korea

[f] School of Medicine, Kangwon National University, Kangwon-do 200-701, Korea

[g] School of Pharmacy, Sungkyunkwan University, Suwon 440-746, Korea

* To whom correspondence should be addressed.

Phone: 82-2-880-7846

Fax: 82-2-888-0649

E-mail: jeewoo@snu.ac.kr

Key Words: Hypoxia Inducible Factor-1, HIF-1, Heat Shock Protein 90, HSP90, Antitumor, Deguelin

Abstract

A series of fluorophenyl and pyridine analogues of **1** and **2** were synthesized as ring-truncated deguelin surrogates and evaluated for their HIF-1α inhibition. Their structure-activity relationship was systematically investigated based on the variation of the linker B-region moiety. Among the inhibitors, compound **25** exhibited potent HIF-1α inhibition in a dose-dependent manner and significant antitumor activity in H1299 with less toxicity than deguelin. It also inhibited *in vitro* hypoxia-mediated angiogenic processes in HRMECs. The docking study indicates that **25** occupied the C-terminal ATP-binding pocket of HSP90 in a similar mode as **1**, which implies that the anticancer and antiangiogenic activities of **25** are derived from HIF-1α destabilization by binding to the C-terminal ATP-binding site of *h*HSP90.

1. Introduction

Hypoxia Inducible Factor-1 (HIF-1) is the transcription factor that regulates the cellular response for the survival of cells in hypoxia. HIF-1 protein is a heterodimer that consists of a constitutively expressed β-subunit and an oxygen-regulated α-subunit. Under normoxia, HIF-1α is degradable by the pVHL-mediated ubiquitin protease pathway, which includes hydroxylation by prolyl hydroxylases (PHD), binding to the product of the von Hippel-Lindau (pVHL), being tagged with polyubiquitin and proteasomal degradation. However, under hypoxia, HIF-1α becomes stable from proline hydroxylation, accumulates and translocates to the nucleus. There, HIF-1α dimerizes with HIF-1β to activate the HIF-1 complex, which binds to hypoxia-response elements (HRE) in the HIF target genes to control transcription. This regulation can induce angiogenesis, proliferation, metastasis and invasion of cancer cells.[1,2] Therefore, the HIF-1α inhibition can inhibit this angiogenesis, decrease the proliferation of cancer cells and reduce the chemotherapy resistance.[3-9] In addition, there has been growing interest in the biology of the HIF-1 pathway and its role in human diseases that are associated with the hypoxic micro-environment, such as cancer, stroke and heart disease.[10-15]

Heat shock protein 90 (HSP90) is a molecular chaperone that regulates the post-translational folding, stability and function of its client proteins such as ErbB2, Src, c-MET, AKT, Raf-1, MMP-2 and HIF-1α. Because the chaperone inhibition can induce the decomposition of HIF-1α, HSP90 inhibition is considered a new and effective therapy against angiogenesis-associated diseases such as cancer. Structurally, the HSP90 protein contains three functional domains: the ATP-binding, protein-binding, and dimerizing domain. Most HSP90 inhibitors that were developed as anticancer agents have been identified as the so-called *N*-term inhibitors, which bind to an ATP-binding domain in the *N*-terminal. However, these inhibitors cause some problems, and one of them induce a heat shock response (HSR), which ultimately leads to an increase in HSP90 and anti-apototic proteins such as HSP70 and HSP27. Therefore, the inhibition of another ATP-binding site

in the C-terminal may be an alternative strategy to discover clinically applicable HSP90 inhibitors.[16-20]

Deguelin, which is a naturally occurring rotenoid, has been reported to prevent tobacco carcinogen-induced lung carcinogenesis by blocking the Akt activation; it also exhibits potent apoptotic and antiangiogenic activities against diverse transformed cells and cancer cells *in vitro* (**Figure 1**).[21] It interferes with the chaperone function of HSP90 by inhibiting ATP binding, which induces the destabilization of HIF-1α and consequent tumor growth reduction in xenograft models of various human cancers.[22]

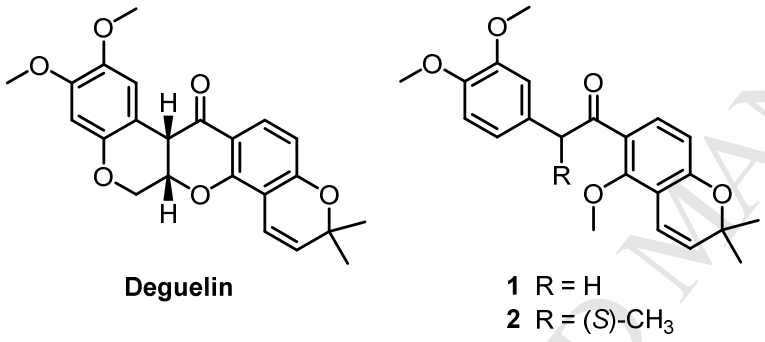

Figure 1. Deguelin and its ring-truncated surrogates

Previously, Chang *et al* reported that two ring-truncated deguelin analogues, compounds **1** and **2**, exhibited excellent HIF-1α suppression and potent cell growth inhibition in the human non-small-cell lung carcinoma cell line, H1299 (**Figure 1**).[23] In addition, their *in vivo* antiangiogenic activities were observed in the zebrafish model in a dose-dependent manner. Jo *et al* also reported that the destabilization of HIF-1α by both compounds suppressed hypoxia-mediated retinal neovascularization and vascular leakage in diabetic retina without inducing a definite toxicity in the oxygen-induced retinopathy mouse model.[24] The results indicated that the new HSP90 inhibitors **1** and **2** were considered promising lead compounds for anti-proliferation and anti-angiogenesis.

Structurally, the ring-truncated deguelin scaffold was divided into three pharmacophoric parts: A-region (3,4-dimethoxyphenyl), B-region (linker), and C-region (2,2-dimethyl chromene ring) (**Figure 2**). To further optimize the leads **1** and **2** as anticancer agents, we decided to investigate their fluorophenyl (X=C-F) and pyridine (X=N) derivatives in the A-region to improve the target binding for the HIF-1α inhibition and aqueous solubility. We presumed that polarizing the 3,4-dimethoxyphenyl group by incorporating a polar nitrogen or fluoro atom might provide better binding interaction to HSP90 and pharmacokinetic profile. In addition, α-methyl carbonyl in the B-region was modified with its bioisosteres, which include olefin, diol, alcohol, and acyl groups (**Figure 2**).

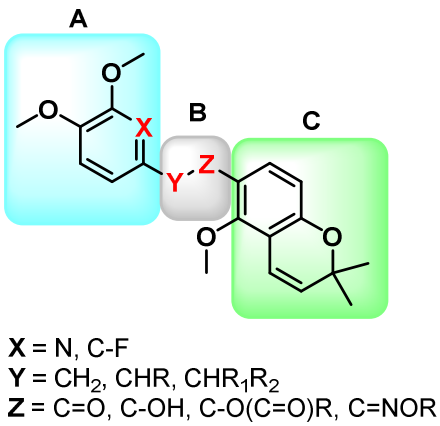

Figure 2. Pharmcophoric regions of the ring-truncated deguelin analogues

In this paper, we investigated the structure activity relationships of the fluorophenyl and pyridine analogues of **1** and **2** for HIF-1α inhibition using western blot assay. With selected potent inhibitors in the series, we further characterized their cytotoxicities in a tumor cell line and anti-angiogenesis in hypoxia-mediated angiogenic processes in human retinal microvascular endothelial cells. In addition, we performed the docking study with HSP90 to determine its mode of action.

2. Result and discussion

2.1. Chemistry

The final compounds were generally synthesized through a carbon-carbon bond formation between the phenyl sulfonyl intermediates of the A-region and 2,2-dimethylchromene aldehyde of the C-region.

To synthesize the phenyl sulfonyl intermediates (**7**, **8**), fluorophenyl aldehyde **3** and pyridine aldehyde **4** as the starting materials were prepared from commercially available o-fluoro catechol and 2-bromo-3-pyridinol, respectively, according to the procedures in the literature.[25,26] The prepared aldehydes (**3**, **4**) were reduced to the corresponding alcohols (**5**, **6**), which were halogenated and subsequently converted into the corresponding sulfonyl intermediates (**7**, **8**), respectively, using benzene sulfinic acid sodium salt (**Scheme 1**). Then, 2,2-Dimethylchromene C-region aldehyde **9**[27] was coupled with the sulfonyl intermediates (**7**, **8**) using n-BuLi to provide two diasteromeric mixtures, which were directly oxidized without separation and subsequently desulfonylated to obtain ketones (**12**, **13**). (**Scheme 2**)

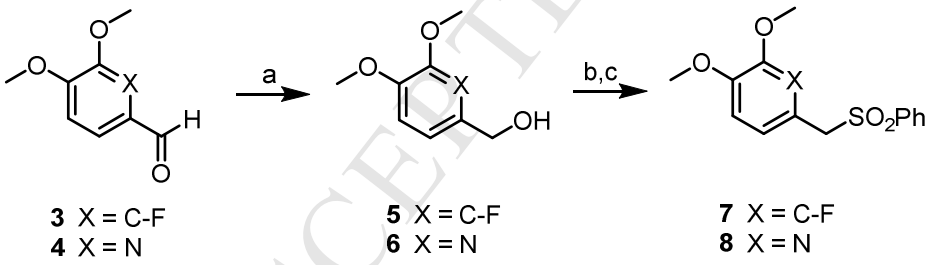

Scheme 1. Synthesis of the A-region
Reagents and conditions: (a) $NaBH_4$, MeOH, 0 °C to rt; (b) $SOCl_2$, MC, 0 °C to rt; (c) $PhSO_2Na$, DMF, rt

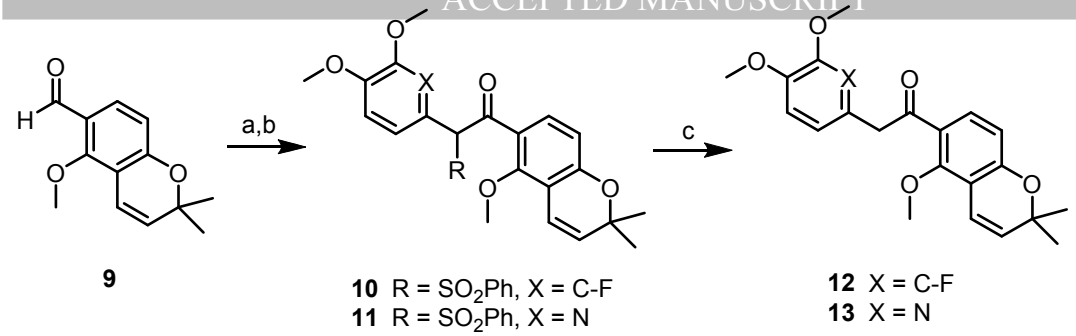

Scheme 2. Synthesis of the ketone analogs
Reagents and conditions: (a) **7** or **8**, n-BuLi, THF, -78 °C; (b) DMP, MC, rt; (c) $(n\text{-}Bu)_3SnH$, AIBN, benzene, reflux

The final alcohol and acyl analogues were synthesized using the conventional routes from the corresponding ketones (**Scheme 3**). Ketones (**12**, **13**) were alkylated with the corresponding alkyl halide to produce α-alkyl ketones (**14-17**), which were reduced by $NaBH_4$ to provide alcohol compounds (**18-23**). Under this condition, the syn diastereomer was found as a predominant isomer (syn:anti=ca. 20:1) when R^1 was a monoalkyl group. For the structural analysis, only **25** (syn) and **26** (anti) were separated, and their stereochemistries were assigned based on the ^{1}H-NMR analysis according to a previous report.[28] The alcohols were further acylated to obtain the acylated products (**24-36**, **41-43**) or carbamoylated in two steps to obtain the carbamoylated products (**37-40**, **44-45**).

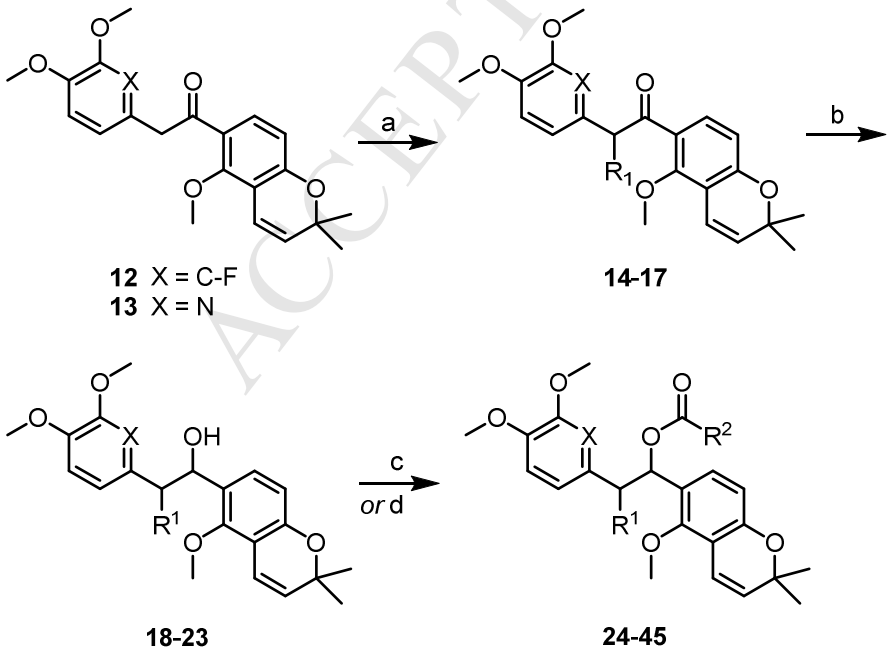

Scheme 3. Syntheses of the alcohol and acyl analogues

Reagents and conditions: (a) R-X, NaH, DMF 0 °C to rt; (b) $NaBH_4$, MeOH, rt; (c) R-COCl, Pyridine, MC, 0°C; (d) i) CDI, MC, 0°C; ii) NH_4OH or NH_2Me or $NHMe_2$, water 40°C

To synthesize the olefinic and dihydroxyl analogues of the B-region, alcohol compounds (**18**, **21**) were dehydrated under acidic condition to provide only trans isomers (**46**, **47**), which were dihydroxylated using OsO_4 to obtain the syn-diol compounds (**48**, **49**). The oxime (**50**) and methyl oxime (**51**) analogues of the pyridine A-region were obtained from ketone **13** (**Scheme 4**).

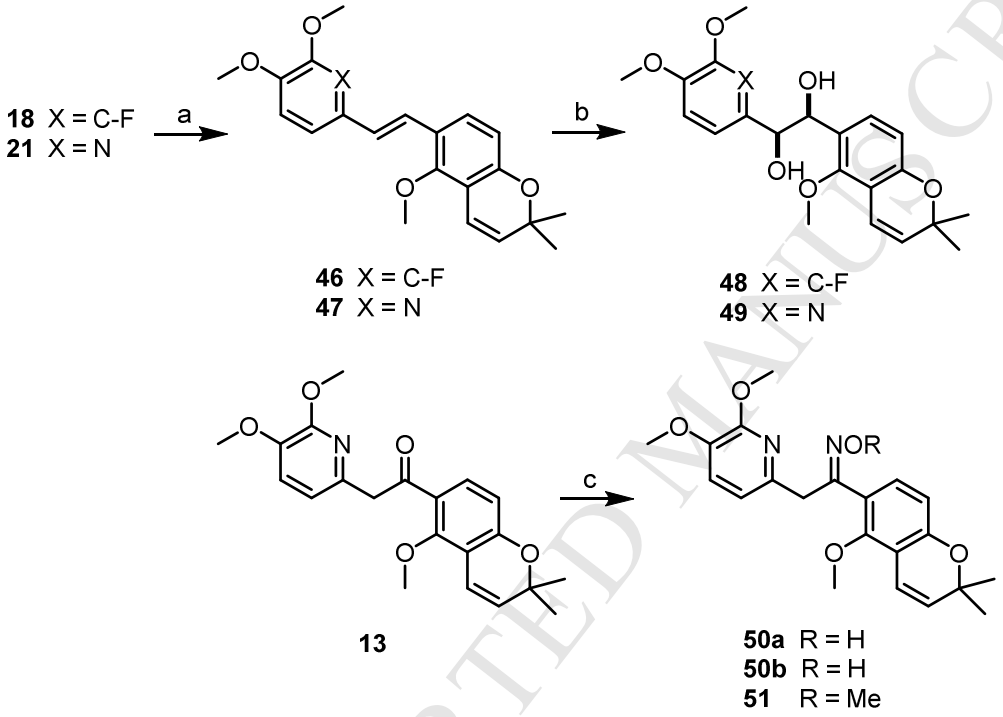

Scheme 4. Syntheses of the olefin, dihydroxy and oxime analogs
Reagents and conditions: (a) p-TSA, toluene, reflux; (b) OsO_4, NMO, acetone, water, rt; (c) NH_2OR-HCl, NaOAc, EtOH, water, reflux

To synthesize the chiral *S*-isomer of **16**, the pyridine surrogate of compound **2**, chiral (*S*)-methyl aldehyde of A-region was prepared from alcohol **6** first (**Scheme 5**). Alcohol **6** was converted to the nitrile and subsequently hydrolyzed to the corresponding acid **52**. Acid **52** was converted to the corresponding (*S*)-oxazolidinone, which was methylated to provide (*S*)-methyl product **53**. Further steps produced the key chiral aldehyde **54** to couple with the C-region. The C-region iodide **56** was synthesized from the corresponding amine **55** by Sandmeyer reaction, which

was prepared from resorcinol as shown in our previous report.[23] The lithiation of iodo compound **56** and subsequent coupling with aldehyde **54** provided the corresponding alcohol, which was oxidized to produce the final chiral (*S*)-methyl ketone **16*S*** (**Scheme 6**).

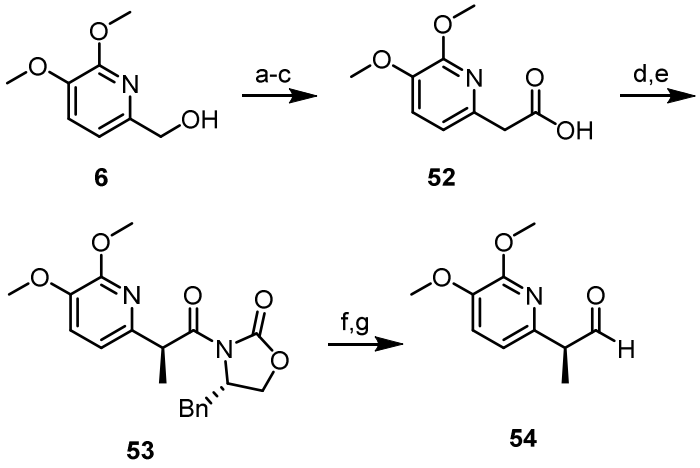

Scheme 5. Synthesis of the chiral A-region of **16*S***
Reagents and conditions: (a) $SOCl_2$, MC, 0 °C to rt; (b) NaCN, DMSO, 60 °C; (c) KOH, EtOH, water, reflux; (d) i) PivCl, TEA, THF, -78 °C; ii) Ax, n-BuLi, THF, -78 °C; (e) LiHMDS, CH_3I, THF, -78 °C; (f) LAH, Et_2O, 0 °C; (g) DMP, MC, rt

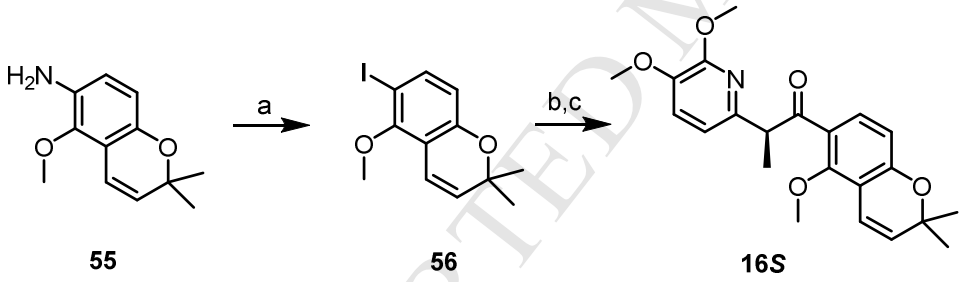

Scheme 6. Synthesis of the chiral **16*S***
Reagents and conditions: (a) $NaNO_2$, KI, c-HCl, H_2O, 0 °C to rt; (b) **54**, n-BuLi, THF, -78 °C; (c) DMP, MC, rt.

2.2. Structure activity relationship for HIF-1α inhibition

The synthesized compounds were evaluated for their HIF-1α inhibition using western blot assay with H1299 cell lines.[23] The H1299 cells were untreated or treated with deguelin and the analogues at 100 nM for 72 h and subsequently incubated under hypoxic conditions for 12 h. The resulting cell lysates were used for the western blot analysis with a monoclonal antibody against HIF-1α. Because all of the compounds have fluorophenyl or pyridine A-region and 2,2-dimethyl

2H-chromene C-region, their inhibitory activities are represented by the structure of the B-region, as shown in **Tables 1-4**.

First, we explored the ketone B-region analogues (**Table 1**). The fluorophenyl and pyridine surrogates (**12**, **13**) of parent **1** showed better HIF-1α inhibition than did parent **1**. Interestingly, the pyridine surrogate (**16*S***) of parent **2** exhibited excellent inhibition, which was ca. 2-fold more potent than **2** and its racemate **16**. **16*S*** also had better activity than deguelin did. This result indicates that the corresponding fluorophenyl and pyridine surrogates are better HIF-1α inhibitors than did the previous ring-truncated deguelin analogues. The analysis indicates that the inhibitory activity increases in the order of no-substituent > α-methyl ≥ α,α'-dimethyl groups next to ketone.

Table 1. Ketone analogues as ring-truncated deguelin

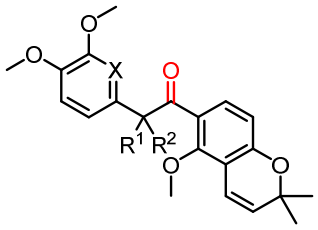

Code	X	R^1, R^2	WB (100 nM)
Deguelin			64
1	C	H, H	85.3
2	C	H, (*S*)-Me	82.1
12	C-F	H, H	67.8 (±37.03)
14	C-F	H, Me	78.6 (±16.44)
15	C-F	Me, Me	74.9 (±6.17)
13	N	H, H	77.6 (±10.86)
16	N	H, Me	89.3 (±11.54)
16*S*	N	H, (*S*)-Me	44.2 (±33.24)
17	N	Me, Me	99.9 (±10.10)

Second, we investigated the alcohol B-region analogues (**Table 2**). Compounds **18** and **19** without substitution at the α-position showed similar inhibitions with the corresponding ketone

analogues (**12**, **13**). However, unlike ketone, the inhibitory activity increased in the order of α,α'-dimethyl > α-methyl > no-substituent next to alcohol.

Table 2. Alcohol analogues as ring-truncated deguelin

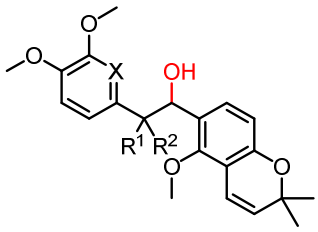

Code	X	R^1, R^2	WB (100 nM)
18	C-F	H, H	74.3 (±33.76)
19	C-F	H, Me	75.0 (±24.20)
20	C-F	Me, Me	68.0 (±33.99)
21	N	H, H	75.2 (±36.33)
22	N	H, Me	71.2 (±29.4)
23	N	Me, Me	69.2 (±19.9)

Third, we examined the O-acyl and O-carbamoyl analogues (**Table 3**). In this series, we incorporated a methyl, ethyl, dimethyl or cyclopropyl group as an α-substituent and acetoxy, propionyloxy, cyclopropanecarbonyloxy, carbamoyloxy, and dimethylcarbamoyloxy as the acyl and carbamoyl groups. All of the α-monoalkyl analogues (**25**, **30**, **33**, **34**, **36**, **38**-**40**, **42**) were syn isomers that were isolated as a predominant form in the B-region. For the SAR analysis, only anti-isomer **26** was separated and found to be much less potent than syn **25**. In this series, the four compounds (**25**, **33**, **38**, **40**) exhibited better activities than did deguelin. Interestingly, all of them had α-methyl moiety next to the O-acyl/carbamate groups, which suggests that a methyl group provided a favorable conformation for the HIF-1α inhibition. A more steric environment at the α-position, such as the ethyl (**34**), dimethyl (**27**, **31**, **35**, **43**, **45**), and cyclopropyl (**28**) groups, diminished the inhibitory activity.

Table 3. Acyl analogues as ring-truncated deguelin

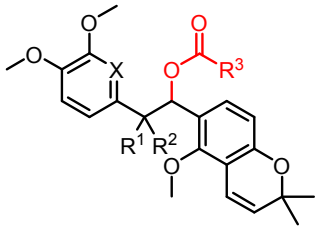

Code	X	R^1, R^2	R^3	WB (100 nM)
24	C-F	H, H	Me	69.3 (±49.85)
25 (Syn)	C-F	H, Me	Me	52.2 (±12.56)
26 (Anti)	C-F	H, Me	Me	79.4 (±5.01)
27	C-F	Me, Me	Me	83.4 (±8.36)
28	C-F	$-CH_2-CH_2-$	Me	154.6 (±17.09)
29	C-F	H, H	Et	77.3 (±39.35)
30	C-F	H, Me	Et	63.7 (±43.72)
31	C-F	Me, Me	Et	88.2 (±16.37)
32	C-F	H, H	Cyclopropyl	70.3 (±19.92)
33	C-F	H, Me	Cyclopropyl	35.0 (±6.05)
34	C-F	H, Et	Cyclopropyl	87.9 (±20.53)
35	C-F	Me, Me	Cyclopropyl	110.6 (±38.89)
36	C-F	H, Me	Cyclobutyl	69.5 (±18.25)
37	C-F	H, H	NH_2	88.9 (±21.10)
38	C-F	H, Me	NH_2	48.8 (±2.99)
39	C-F	H, Me	NHMe	76.5 (±28.37)
40	C-F	H, Me	NMe_2	64.1 (±20.46)
41	N	H, H	Me	114.0 (±27.98)
42	N	H, Me	Me	96.7 (±19.97)
43	N	Me, Me	Me	113.2 (±6.43)
44	N	H, H	NH_2	75.0 (±18.08)
45	N	Me, Me	NH_2	107.7 (±25.14)

Finally, we examined olefin, diol, and oxime B-region analogues (**Table 4**). Although the olefinic derivatives (**46**, **47**) did not show any HIF-1α inhibition, the diol derivatives (**48**, **49**) exhibited good HIF-1α inhibition, which was comparable to that of deguelin. **48** and **49** had better

activity than did their corresponding mono-hydroxyl surrogates (**18**, **21**) and similar activity to the ketone surrogates (**12**, **13**). In addition, the methyl oxime derivative of pyridine A-region (**51**) displayed excellent inhibition, which was better than deguelin, but its oxime isomers (**50**) showed moderate inhibition.

Table 4. Olefin, diol and oxime analogues as ring-truncated deguelin

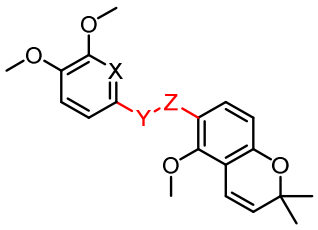

Code	X	Y, Z	WB (100 nM)
46	C-F	-CH=CH-	133.8 (±40.03)
47	N	-CH=CH-	133.2 (±24.03)
48	C-F	-CH(OH)-CH(OH)-	68.1 (±4.23)
49	N	-CH(OH)-CH(OH)-	68.9 (±1.46)
50a	N	-CH_2-C(=NOH)-	78.5 (±25.36)
50b	N	-CH_2-C(=NOH)-	79.2 (±34.62)
51	N	-CH_2-C(=$NOCH_3$)-	64.8 (±19.78)

Among the tested compounds, we selected 6 compounds with better HIF-1α inhibition than deguelin and evaluated their inhibition at a low concentration (10 nM) to examine the dose-dependent inhibition (**Table 5**). As expected, all of the selected compounds showed better inhibition than deguelin at 10 nM. In particular, compound **25** showed the best inhibition.

Table 5. HIF-1α inhibition of the selected potent compounds

	WB (10 nM)	WB (100 nM)
Deguelin	94.0	64
16*S*	88.4 (±11.53)	44.2 (±33.24)
25	63.2 (±17.53)	52.2 (±12.56)
33	81.6 (±22.07)	35.0 (±6.05)

38	80.9 (±12.67)	48.8 (±2.99)
40	93.6 (±10.89)	64.1 (±20.46)
51	74.0 (±4.75)	64.8 (±19.78)

2.3. Antitumor activity

Deguelin and its analogs exhibited profound antiproliferative effects on human malignant bronchial epithelial cells and *in vivo* efficacy in suppressing the lung tumor formation in the mice model, which indicates that they are promising antitumor candidates for lung cancer.[21,22] In this regard, the two compounds **25** and **33**, which were selected based on the primary HIF-1α inhibition screening result, were tested for antitumor activity in the human non-small-cell lung carcinoma cell (H1299) line using the MTT assay (**Figure 3**). As expected, both compounds showed promising cytotoxicity in a concentration-dependent manner, where the viability of the cell was reduced to 50% at 20 μM. The result indicates that the cytotoxicities are derived from their HIF-1α inhibition.

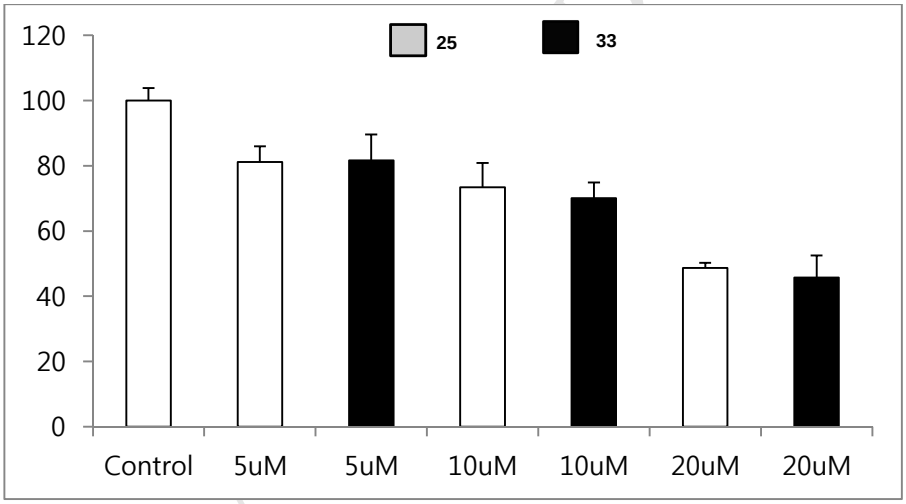

Figure 3. Antitumor activity of **25** and **33** in H1299

Because the use of deguelin as anticancer agents is limited because of its potential toxicities, we examined the toxicity of **25** by testing the effect of **25** on the viability of hippocampal

cell (HT-22). Compared to deguelin, compound **25** showed significantly reduced cytotoxicity, which indicates that **25** is a more potent and less toxic antitumor agent than deguelin (**Figure 4**).

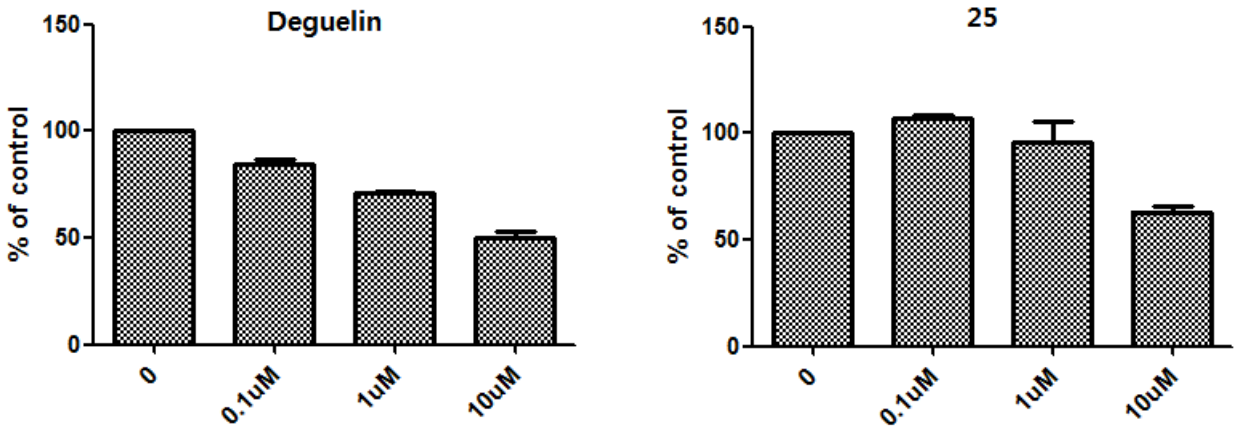

Figure 4. Effect of deguelin and **25** on the viability of mouse hippcampus (HT-22)

2.4. Anti-angiogenesis activity

Angiogenesis is the formation of new blood vessels, which are a significant component of a solid tumor for its proliferation and metastasis. The VEGF (vascular endothelial growth factor) plays a pivotal role in tumor angiogenesis and is up-regulated in tumor cells under hypoxic conditions.

The anti-angiogenesis activity of compound **25** was examined using proliferation and migration assays in human retinal microvascular endothelial cells (HRMECs), which were previously described[29], and compared to deguelin at each 100 nM (**Figure 5**). Although the VEGF activated angiogenesis in the proliferation and migration assays, compound **25** effectively inhibited the *in vitro* hypoxia-mediated angiogenic processes in both assays at a comparable level to deguelin, which indicates that it can be used as a potential anti-angiogenic agent to suppress the retinal neovascularization for the treatment of diabetic retinopathy.

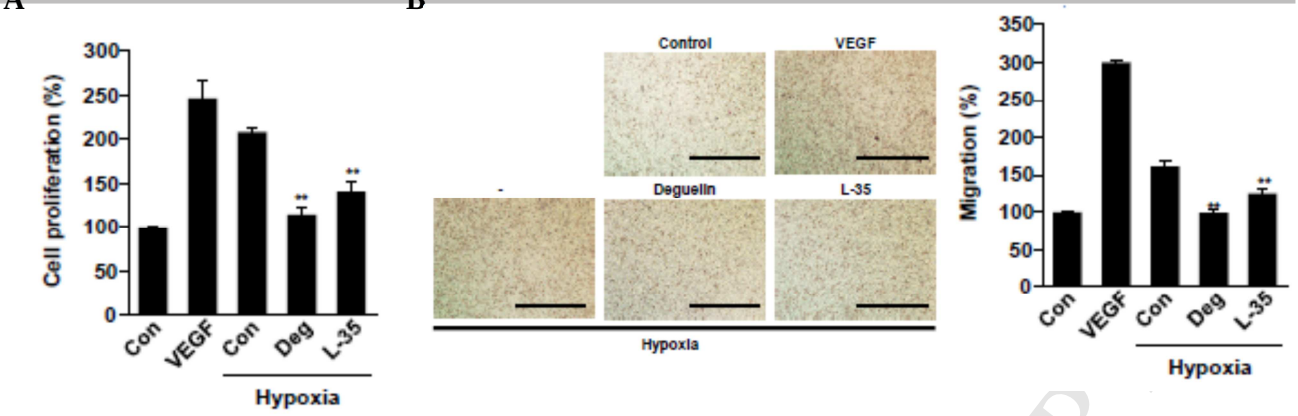

Figure 5. Anti-angiogenesis activity of **25** in HRMECs (A: proliferation assay; B: migration assay)

2.5. Molecular Modeling

We recently demonstrated that L80 (**Figure 6D**), which is a cyclized analogue of compound **25** , strongly diminished the physical interaction between HIF-1α and HSP90 in H1299 cells by directly modulating the function of HSP90 using co-immunoprecipitation and pull-down assays.[30] In addition, we showed that L80 could bind to the C-terminal ATP-binding pocket of HSP90 to hamper the HSP90 function when we studied recombinant HSP90 proteins, which contain the full-length protein, N-terminal/middle domain, middle domain, and C-terminal domain. Furthermore, our recent study confirmed that lead **1** also bound to the C-terminal ATP-binding pocket of HSP90, disrupted the HSP90 function and caused a degradation of client proteins without affecting the HSP70 expression (unpublished data). These data suggest that compound **25** inhibits the HSP90 function by binding to the C-terminal ATP-binding pocket of HSP90.

To ensure the binding of **25** to the C-terminal ATP-binding pocket of HSP90 for the HIF-1α inhibition, we performed a docking study of **25** in the C-terminal ATP-binding pocket of *h*HSP90 homodimer (**Figure 6**). The active site was determined based on the reported *h*HSP90 C-terminal ATP-binding site.[31] To examine the docking poses, we conducted a docking study of **25** in the C-terminal ATP-binding pocket of the *h*HSP90 homodimer. The C-terminal ATP-binding site was assigned as an active site at the dimerization interface (**Figure 6C**). After docking, we

compared the docking pose and score of ATP with those of **25**. **Figure 6A** shows that ATP (white carbon) fits well into the ATP-binding pocket of chain A. The adenine ring is located deep into the hydrophobic pocket. The phosphate moiety interacts with multiple hydrogen bonds with Glu611, and 3´-hydroxy of the sugar moiety interacts with Ser677 in chain A via a hydrogen bond. Compound **25** is partially superimposed with the sugar-phosphate moiety of ATP. However, **25** binds to the active site with a higher docking score ($-\log K_d = 7.80$) than ATP ($-\log K_d = 6.29$). **25** occupies the centre of the active site by forming multiple hydrogen bonds with both chains A and B (**Figure 6B** and **6C**). The oxygen atom of the methoxy group that is attached to the 2,2-dimethyl chromene ring forms a hydrogen bond with the side chain NH of Lys 615 in chain A, which is part of the ATP-binding pocket. Two oxygen atoms of the acetoxy group form hydrogen bonds with the side chain of Lys615 in chain B. Furthermore, the substituents of the 3,4-dimethoxy-2-fluorophenyl group are involved in forming hydrogen bonding networks. The fluoro group and oxygen atom of 3-methoxy form hydrogen bonds with Lys615 in chain B. The oxygen atom of 4-methoxy interacts with sidechain NH of Asn 622 (chain B). Hugel and coworkers reported that the role of the C-terminal inhibitors is to prohibit the global conformational changes, which include N-terminal dimerization and the formation of the ATP binding pocket.[32-35] Our docking results demonstrate that **25** can compete with ATP in binding to the C-terminal ATP binding site and stabilize the open state of C-terminal *h*HSP90 with the bridging hydrogen bond networks at the interface of the homodimer.

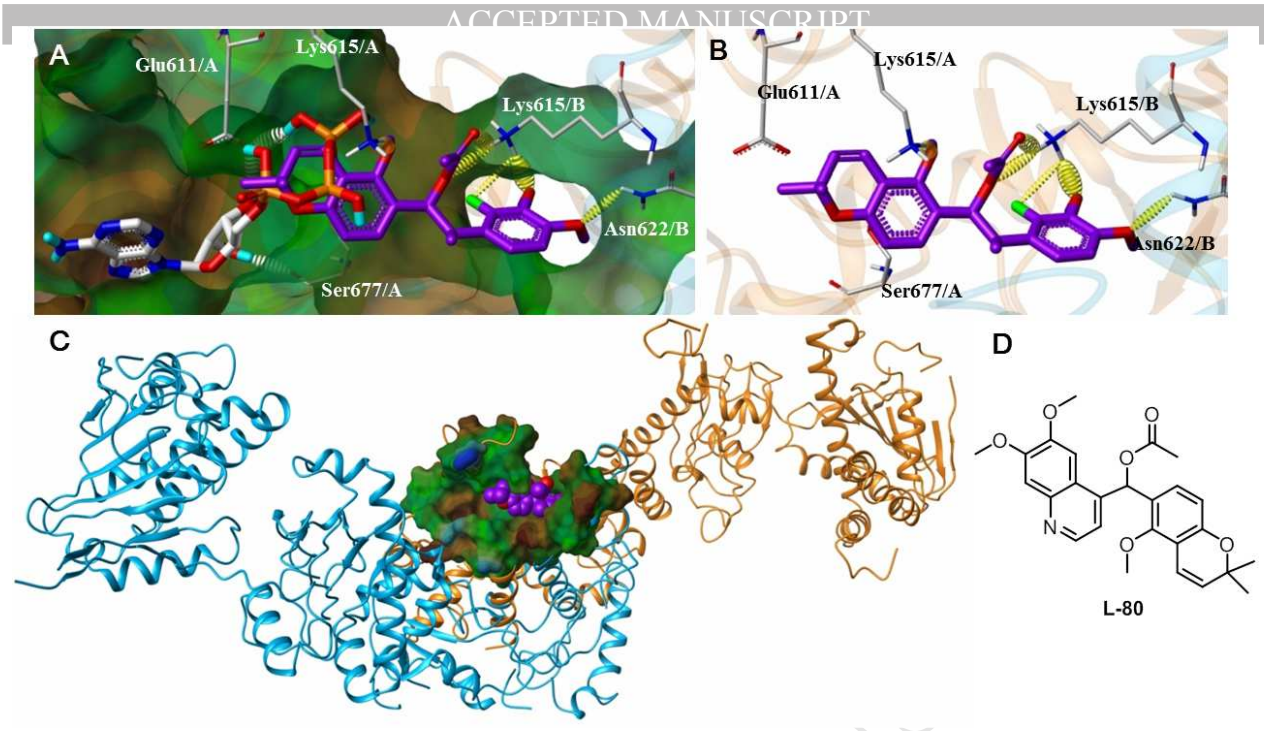

Figure 6. Molecular modeling of **25**
(A) Overlay of the docking pose of **25** (purple carbon) and ATP (white carbon) in the active site of the hHsp90 C-terminal. The key amino acid residues of the binding site are represented by the grey carbon capped stick. The active site is shown as a lipophilicity property surface map (brown colour: hydrophobic; blue colour: hydrophilic) (B) Docked pose of **25**. The dashed ellipsoids are hydrogen-bonding interactions (<2.8 Å). A and B indicate the chain names. (C) Binding site for **25** in the dimerization interface of the open state hHsp90. **25** is represented by the purple CPK model. Chain A is shown as an orange ribbon, and chain B is a cyan ribbon. (D) Structure of L-80

3. Conclusion

A series of fluorophenyl and pyridine analogues of **1** and **2**, which are lead HIF-1α inhibitors through HSP90 inhibition as ring-truncated deguelin surrogates, were investigated for their HIF-1α inhibition. Their structure-activity relationship was systematically examined by varying the B-region moiety. Among the studied inhibitors, 6 compounds showed better HIF-1α inhibition than deguelin. The two selected inhibitors, **25** and **33**, exhibited promising antitumor activity in human non-small cell lung carcinoma (H1299). In addition, compound **25** inhibited *in vitro* hypoxia-mediated angiogenic processes in human retinal microvascular endothelial cells (HRMECs). The docking study of **25** with the *h*HSP90 C-terminal ATP-binding site indicated that **25** snugly bound to the C-terminal ATP-binding pocket of the *h*HSP90 homodimer with a high docking score, as found in its cyclized analog L80. Overall, compound **25** is a potential anticancer

and antiangiogenic agent with an HIF-1α inhibition mechanism through binding to the C-terminal ATP-binding site of *h*HSP90.

Acknowledgments

This work was supported by grants from the National Research Foundation of Korea (NRF), the Ministry of Science, Republic of Korea (NRF-20110019400).

Appendix A. Supplementary data

Supplementary data related to this article can be found at

References and notes

[1] Q. Ke, M. Costa, Hypoxia-inducible factor-1 (HIF-1), Molecular pharmacology, 70 (2006) 1469-1480.

[2] M. Yee Koh, T.R. Spivak-Kroizman, G. Powis, HIF-1 regulation: not so easy come, easy go, Trends in biochemical sciences, 33 (2008) 526-534.

[3] G.L. Semenza, Targeting HIF-1 for cancer therapy, Nature reviews. Cancer, 3 (2003) 721-732.

[4] Hua Zhong, Angelo M. De Marzo, Erik Laughner, Michael Lim, David A. Hilton, David Zagzag, Peter Buechler,William B. Isaacs, Gregg L. Semenza, Jonathan W. Simons, Overexpression of Hypoxia-inducible Factor 1α in Common Human Cancers and Their Metastases, Cancer Res. 59 (1999) 5830–5835.

[5] K.L. Talks, H. Turley, K.C. Gatter, P.H. Maxwell, C.W. Pugh, P.J. Ratcliffe, A.L. Harris, The Expression and Distribution of the Hypoxia-Inducible Factors HIF-1α and HIF-2α in Normal

Human Tissues, Cancers, and Tumor-Associated Macrophages, The American Journal of Pathology, 157 (2000) 411-421.

[6] N. J. P. Beasley, R. Leek, M. Alam, H. Turley, G. J. Cox, K. Gatter, P. Millard, S. Fuggle, A. L. Harris, Hypoxia-inducible Factors HIF-1α and HIF-2α in Head and Neck Cancer: Relationship to Tumor Biology and Treatment Outcome in Surgically Resected Patients, Cancer Res. 62 (2002), 2493–2497.

[7] M. Volm, R. Koomagi, Hypoxia-inducible factor (HIF-1) and its relationship to apoptosis and proliferation in lung cancer, Anticancer Res. 20 (2000**)** 1527–1533.

[8] P. Birner, M. Schindl, A. Obermair, G. Breitenecker, G. Oberhuber, Expression of Hypoxia-inducible Factor 1α in Epithelial Ovarian Tumors: Its Impact on Prognosis and on Response to Chemotherapy, Clin. Cancer Res. 7 (2001) 1661–1668.

[9] M. I. Koukourakis, A. Giatromanolaki, J. Skarlatos, L. Corti, S. Blandamura, M. Piazza, K. C. Gatter, A. L. Harris, Hypoxia Inducible Factor (HIF-1α and HIF-2α) Expression in Early Esophageal Cancer and Response to Photodynamic Therapy and Radiotherapy, Cancer Res. 61 (2001) 1830–1832.

[10] A. Unruh, A. Ressel, H.G. Mohamed, R.S. Johnson, R. Nadrowitz, E. Richter, D.M. Katschinski, R.H. Wenger, The hypoxia-inducible factor-1 alpha is a negative factor for tumor therapy, Oncogene, 22 (2003) 3213-3220.

[11] D. M. Aebersold, P. Burri, K. T. Beer, J. Laissue, V. Djonov, R. H. Greiner, G. L. Semenza, Expression of Hypoxia-inducible Factor-1α: A Novel Predictive and Prognostic Parameter in the Radiotherapy of Oropharyngeal Cancer, Cancer Res. 61 (2001) 2911–2916.

[12] A. Rapisarda, B. Uranchimeg, D. A. Scudiero, M. Selby, E. A. Sausville, R. H. Shoemaker, G. Melillo, Identification of Small Molecule Inhibitors of Hypoxia-inducible Factor 1 Transcriptional Activation Pathway Cancer Res. 62 (2002) 4316–4324.

[13] E-J. Yeo, Y-S. Chun, Y-S. Cho, J. Kim, J-C. Lee, M-S. Kim, J-W. Park, YC-1: A Potential Anticancer Drug Targeting Hypoxia-Inducible Factor 1, J. Natl Cancer Inst. 95, (2003), 516–525.

[14] S. J. Welsh, R. R. Williams, A. Birmingham, D. J. Newman, D. L. Kirkpatrick, G. Powis, The Thioredoxin Redox Inhibitors 1-Methylpropyl 2-Imidazolyl Disulfide and Pleurotin Inhibit Hypoxia-induced Factor 1α and Vascular Endothelial Growth Factor Formation, Mol. Cancer Ther. 2 (2003) 235–243.

[15] J-W. Lee, S-H. Bae, J-W. Jeong, S-H. Kim, K-W. Kim, Hypoxia-inducible factor (HIF-1)α: its protein stability and biological functions, Exp. Mol. Med. 1 (2004) 1-12.

[16] Y. Xia, H.K. Choi, K. Lee, Recent advances in hypoxia-inducible factor (HIF)-1 inhibitors, European journal of medicinal chemistry, 49 (2012) 24-40.

[17] J.C. Young, V.R. Agashe, K. Siegers, F.U. Hartl, Pathways of chaperone-mediated protein folding in the cytosol, Nature reviews. Molecular cell biology, 5 (2004) 781-791.

[18] L. Neckers, P. Workman, Hsp90 molecular chaperone inhibitors: are we there yet?, Clinical cancer research : an official journal of the American Association for Cancer Research, 18 (2012) 64-76.

[19] L. Whitesell, S.L. Lindquist, HSP90 and the chaperoning of cancer, Nature reviews. Cancer, 5 (2005) 761-772.

[20] R. Bagatell, L. Whitesell, Altered Hsp90 function in cancer: A unique therapeutic opportunity, Mol. Cancer Ther. 3 (2004) 1021−1030.

[21] (a) J. Beliakoff, R. Bagatell, G. Paine-Murrieta, C.W. Taylor, A. E. Lykkesfeldt, L. Whitesell, Hormone-Refractory Breast Cancer Remains Sensitive to the Antitumor Activity of Heat Shock Protein 90 Inhibitors, Clin. Cancer Res. 9 (2003) 4961−4971. (b) B.K. Eustace, T. Sakurai, J.K. Stewart, D. Yimlamai, C. Unger, C. Zehetmeier, B. Lain, C. Torella, S.W. Henning, G. Beste, B.T. Scroggins, L. Neckers, L.L. Ilag, D.G. Jay, Functional proteomic screens reveal an essential extracellular role for hsp90 alpha in cancer cell invasiveness, Nature cell biology, 6 (2004) 507-514. (c) L. Stepanova, X. Leng, S. B. Parker, J. W. Harper, Mammalian $p50^{Cdc37}$ is a protein kinase targeting subunit of Hsp90 that binds and stabilizes Cdk4 Gene. Dev. 10 (1996) 1491−1502. (d) S. E. Holt, D. L. Aisner, Joseph Baur, V. M. Tesmer, M. Dy, M. Ouellette, J. B. Trager, G. B. Morin,

D. O. Toft, J. W. Shay, W. E. Wright, M. A. White, Functional requirement of p23 and Hsp90 in telomerase complexes, Genes Dev. 13 (1999) 817−826. (e) P. N. Mu¨ nster, D. C. Marchion, A. D. Basso, N. Rosen, Degradation of HER2 by Ansamycins Induces Growth Arrest and Apoptosis in Cells with HER2 Overexpression via a HER3, phosphatidylinositol 3'-Kinase-AKT-dependent Pathway, Cancer Res. 62 (2002) 3132−3137. (f) A.D. Basso, D.B. Solit, G. Chiosis, B. Giri, P. Tsichlis, N. Rosen, Akt forms an intracellular complex with heat shock protein 90 (Hsp90) and Cdc37 and is destabilized by inhibitors of Hsp90 function, The Journal of biological chemistry, 277 (2002) 39858-39866. (g) J.S. Isaacs, Y.J. Jung, E.G. Mimnaugh, A. Martinez, F. Cuttitta, L.M. Neckers, Hsp90 regulates a von Hippel Lindau-independent hypoxia-inducible factor-1 alpha-degradative pathway, J. Biol. Chem., 277 (2002) 29936-29944.

[22] S.H. Oh, J.K. Woo, Y.D. Yazici, J.N. Myers, W.Y. Kim, Q. Jin, S.S. Hong, H.J. Park, Y.G. Suh, K.W. Kim, Structural basis for depletion of heat shock protein 90 client proteins by deguelin. J. Natl. Cancer Inst., 99 (2007) 949−961.

[23] D.J. Chang, H. An, K.S. Kim, H.H. Kim, J. Jung, J.M. Lee, N.J. Kim, Y.T. Han, H. Yun, S. Lee, G. Lee, S. Lee, J.S. Lee, J.H. Cha, J.H. Park, J.W. Park, S.C. Lee, S.G. Kim, J.H. Kim, H.Y. Lee, K.W. Kim, Y.G. Suh, Design, synthesis, and biological evaluation of novel deguelin-based heat shock protein 90 (HSP90) inhibitors targeting proliferation and angiogenesis, J. Med. Chem., 55 (2012) 10863-10884.

[24] D.H. Jo, H. An, D.J. Chang, Y.Y. Baek, C.S. Cho, H.O. Jun, S.J. Park, J.H. Kim, H.Y. Lee, K.W. Kim, J. Lee, H.J. Park, Y.M. Kim, Y.G. Suh, J.H. Kim, Hypoxia-mediated retinal neovascularization and vascular leakage in diabetic retina is suppressed by HIF-1alpha destabilization by SH-1242 and SH-1280, novel hsp90 inhibitors, Journal of molecular medicine, 92 (2014) 1083-1092.

[25] A. Adejare, F. Gusovsky, W. Padgett, C. R. Creveling, J. W. Daly, K. L. Kirk, Syntheses and Adrenergic Activities of Ring-Fluorinated Epinephrines, J. Med. Chem. 31 (1988) 1972-1977.

[26] C. Nemecek, W.A. Metz, S. Wentzler, F.X. Ding, C. Venot, C. Souaille, A. Dagallier, S. Maignan, J.P. Guilloteau, F. Bernard, A. Henry, S. Grapinet, D. Lesuisse, Design of potent IGF1-R inhibitors related to bis-azaindoles, Chemical biology & drug design, 76 (2010) 100-106.

[27] G.E. Henry, H. Jacobs, A short synthesis of 5-methoxy-2,2,-dimethyl-2H-1-benzopyran-6-propanoic acid methyl ester, Tetrahedron, 57 (2001) 5335-5338.

[28] N. Matsumori, D. Kaneno, M. Murata, H. Nakamura, K. Tachibana, Stereochemical determination of acyclic structures based on carbon-proton spin-coupling constants. A method of configuration analysis for natural product, J. Org. Chem., 64 (1999) 866-876.

[29] C.K. Kim, Y.K. Choi, H. Lee, K.S. Ha, M.H. Won, Y.G. Kwon, Y.M. Kim, The farnesyltransferase inhibitor LB42708 suppresses vascular endothelial growth factor-induced angiogenesis by inhibiting ras-dependent mitogen-activated protein kinase and phosphatidylinositol 3-kinase/Akt signal pathways, Molecular pharmacology, 78 (2010) 142-150.

[30] S-C. Lee, H-Y. Min, H. Choi, H. S. Kim, K-C. Kim, S-J. Park, M. A. Seong, J. H. Seo, H-J. Park, Y-G. Suh, K-W, Kim, J. Lee, H-Y. Lee, Synthesis and Evaluation of a Novel Deguelin Derivative, L80, which Disrupts ATP Binding to the C-terminal Domain of Heat Shock Protein 90, Mol. Pharm. 88 (2015) 245-255.

[31] (a) M. Sgobba, G. Degliesposti, A.M. Ferrari, G. Rastelli, Structural models and binding site prediction of the C-terminal domain of human Hsp90: a new target for anticancer drugs, Chemical biology & drug design, 71 (2008) 420-433. (b) M. Sgobba, R. Forestiero, G. Degliesposti, G. Rastelli, Exploring the Binding Site of C-Terminal Hsp90 Inhibitors, Journal of Chemical Information and Modeling, 50 (2010) 1522-1528.

[32] C. Soti, A. Racz, P. Csermely, A Nucleotide-dependent molecular switch controls ATP binding at the C-terminal domain of Hsp90. N-terminal nucleotide binding unmasks a C-terminal binding pocket, The Journal of biological chemistry, 277 (2002) 7066-7075.

[33] C. Garnier, D. Lafitte, P.O. Tsvetkov, P. Barbier, J. Leclerc-Devin, J.M. Millot, C. Briand, A.A. Makarov, M.G. Catelli, V. Peyrot, Binding of ATP to heat shock protein 90: evidence for an

ATP-binding site in the C-terminal domain, The Journal of biological chemistry, 277 (2002) 12208-12214.

[34] A.K. Shiau, S.F. Harris, D.R. Southworth, D.A. Agard, Structural Analysis of E. coli hsp90 reveals dramatic nucleotide-dependent conformational rearrangements, Cell, 127 (2006) 329-340.

[35] C. Ratzke, M. Mickler, B. Hellenkamp, J. Buchner, T. Hugel, Dynamics of heat shock protein 90 C-terminal dimerization is an important part of its conformational cycle, PNAS, 107 (2010) 16101-16106.

Legends

Figure 1. Deguelin and its ring-truncated surrogates

Figure 2. Pharmcophoric regions of the ring-truncated deguelin analogues

Scheme 1. Synthesis of the A-region

Scheme 2. Synthesis of the ketone analogs

Scheme 3. Syntheses of the alcohol and acyl analogues

Scheme 4. Syntheses of the olefin, dihydroxy and oxime analogs

Scheme 5. Synthesis of the chiral A-region of 16*S*

Scheme 6. Synthesis of the chiral 16*S*

Table 1. Ketone analogues as ring-truncated deguelin

Table 2. Alcohol analogues as ring-truncated deguelin

Table 3. Acyl analogues as ring-truncated deguelin

Table 4. Olefin, diol and oxime analogues as ring-truncated deguelin

Table 5. HIF-1α inhibition of the selected potent compounds

Figure 3. Antitumor activity of **25** and **33** in H1299

Figure 4. Effect of deguelin and **25** on the viability of mouse hippcampus (HT-22)

Figure 5. Anti-angiogenesis activity of **25** in HRMECs

Figure 6. Molecular modeling of **25**

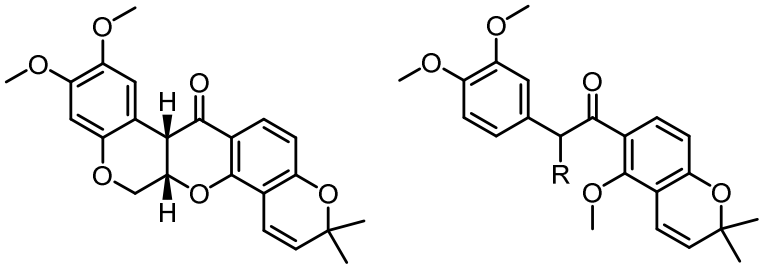

Figure 1. Deguelin and its ring-truncated surrogates

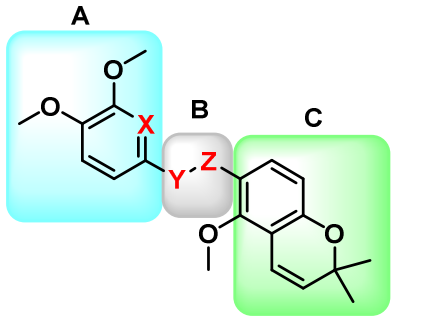

Figure 2. Pharmcophoric regions of the ring-truncated deguelin analogues

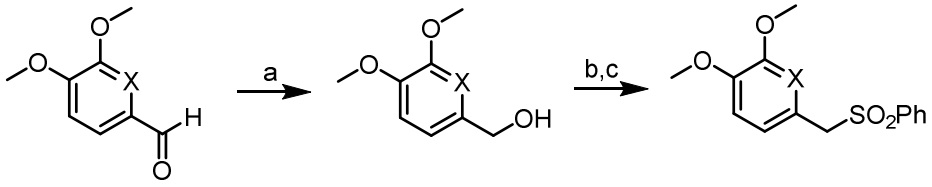

3 X = C-F
4 X = N

5 X = C-F
6 X = N

7 X = C-F
8 X = N

Scheme 1. Synthesis of the A-region
Reagents and conditions: (a) $NaBH_4$, MeOH, 0 °C to rt; (b) $SOCl_2$, MC, 0 °C to rt; (c) $PhSO_2Na$, DMF, rt

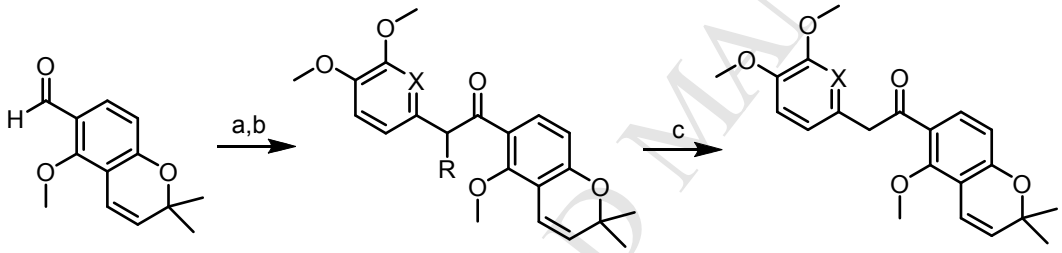

9

10 R = SO_2Ph, X = C-F
11 R = SO_2Ph, X = N

12 X = C-F
13 X = N

Scheme 2. Synthesis of the ketone analogs
Reagents and conditions: (a) **7** or **8**, n-BuLi, THF, -78 °C; (b) DMP, MC, rt; (c) $(n\text{-}Bu)_3SnH$, AIBN, benzene, reflux

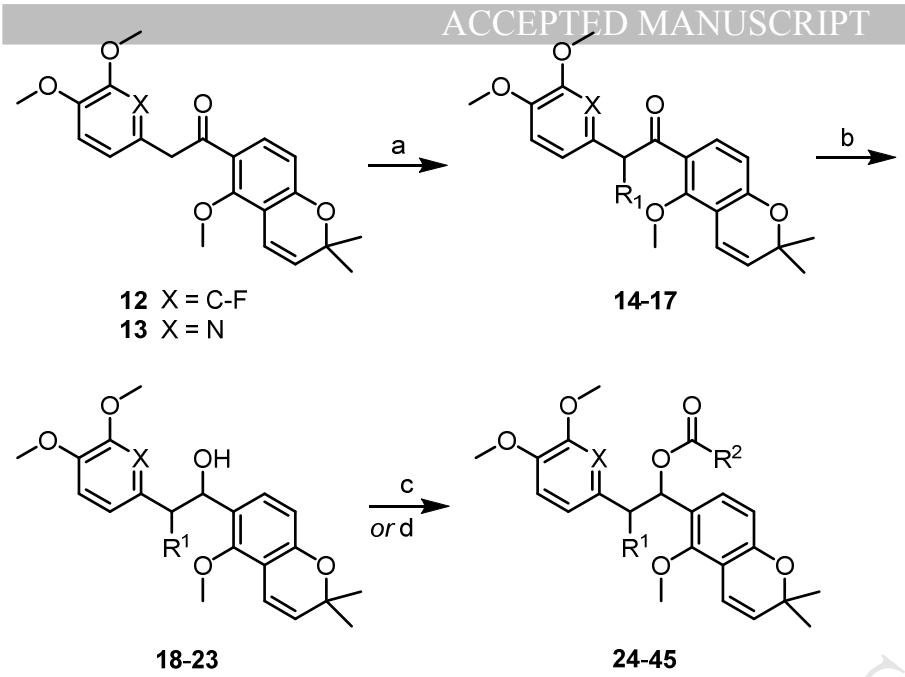

Scheme 3. Syntheses of the alcohol and acyl analogues
Reagents and conditions: (a) R-X, NaH, DMF 0 °C to rt; (b) $NaBH_4$, MeOH, rt; (c) R-COCl, Pyridine, MC, 0°C; (d) i) CDI, MC, 0°C; ii) NH_4OH or NH_2Me or $NHMe_2$, water 40°C

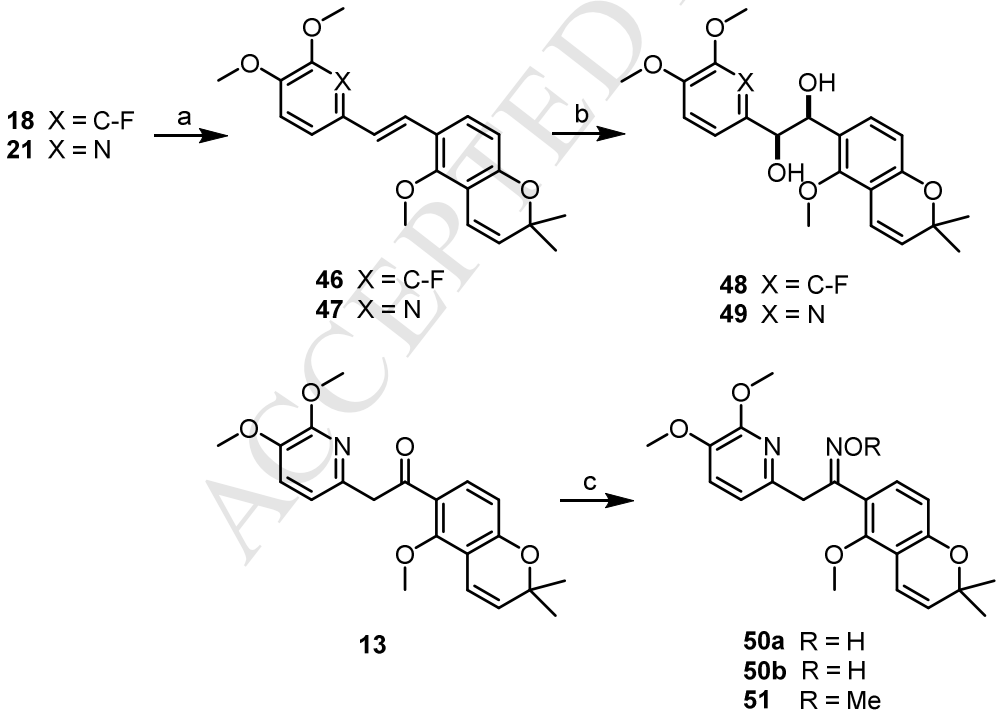

Scheme 4. Syntheses of the olefin, dihydroxy and oxime analogs
Reagents and conditions: (a) p-TSA, toluene, reflux; (b) OsO_4, NMO, acetone, water, rt; (c) NH_2OR-HCl, NaOAc, EtOH, water, reflux

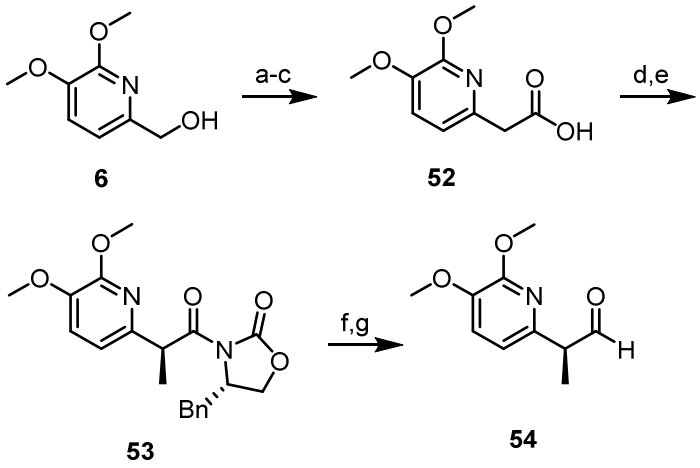

Scheme 5. Synthesis of the chiral A-region of **16*S***
Reagents and conditions: (a) $SOCl_2$, MC, 0 °C to rt; (b) NaCN, DMSO, 60 °C; (c) KOH, EtOH, water, reflux; (d) i) PivCl, TEA, THF, -78 °C; ii) Ax, n-BuLi, THF, -78 °C; (e) LiHMDS, CH_3I, THF, -78 °C; (f) LAH, Et_2O, 0 °C; (g) DMP, MC, rt

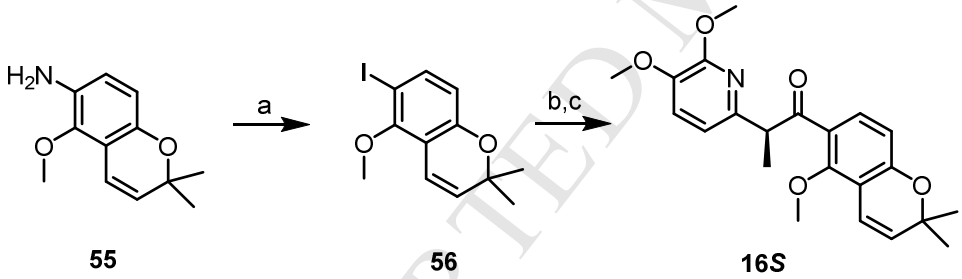

Scheme 6. Synthesis of the chiral **16*S***
Reagents and conditions: (a) $NaNO_2$, KI, c-HCl, H_2O, 0 °C to rt; (b) **54**, n-BuLi, THF, -78 °C; (c) DMP, MC, rt.

Table 1. Ketone analogues as ring-truncated deguelin

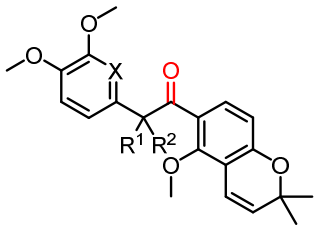

Code	X	R^1, R^2	WB (100 nM)
Deguelin			64
1	C	H, H	85.3
2	C	H, (*S*)-Me	82.1
12	C-F	H, H	67.8 (±37.03)
14	C-F	H, Me	78.6 (±16.44)
15	C-F	Me, Me	74.9 (±6.17)
13	N	H, H	77.6 (±10.86)
16	N	H, Me	89.3 (±11.54)
16*S*	N	H, (*S*)-Me	44.2 (±33.24)
17	N	Me, Me	99.9 (±10.10)

Table 2. Alcohol analogues as ring-truncated deguelin

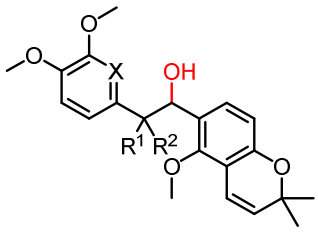

Code	X	R^1, R^2	WB (100 nM)
18	C-F	H, H	74.3 (±33.76)
19	C-F	H, Me	75.0 (±24.20)
20	C-F	Me, Me	68.0 (±33.99)
21	N	H, H	75.2 (±36.33)
22	N	H, Me	71.2 (±29.4)
23	N	Me, Me	69.2 (±19.9)

Table 3. Acyl analogues as ring-truncated deguelin

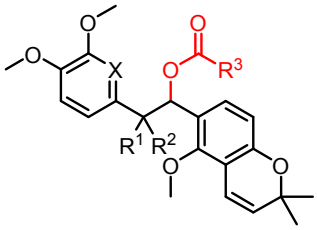

Code	X	R^1, R^2	R^3	WB (100 nM)
24	C-F	H, H	Me	69.3 (±49.85)
25 (Syn)	C-F	H, Me	Me	52.2 (±12.56)
26 (Anti)	C-F	H, Me	Me	79.4 (±5.01)
27	C-F	Me, Me	Me	83.4 (±8.36)
28	C-F	$-CH_2-CH_2-$	Me	154.6 (±17.09)
29	C-F	H, H	Et	77.3 (±39.35)
30	C-F	H, Me	Et	63.7 (±43.72)
31	C-F	Me, Me	Et	88.2 (±16.37)
32	C-F	H, H	Cyclopropyl	70.3 (±19.92)
33	C-F	H, Me	Cyclopropyl	35.0 (±6.05)
34	C-F	H, Et	Cyclopropyl	87.9 (±20.53)
35	C-F	Me, Me	Cyclopropyl	110.6 (±38.89)
36	C-F	H, Me	Cyclobutyl	69.5 (±18.25)
37	C-F	H, H	NH_2	88.9 (±21.10)
38	C-F	H, Me	NH_2	48.8 (±2.99)
39	C-F	H, Me	NHMe	76.5 (±28.37)
40	C-F	H, Me	NMe_2	64.1 (±20.46)
41	N	H, H	Me	114.0 (±27.98)
42	N	H, Me	Me	96.7 (±19.97)
43	N	Me, Me	Me	113.2 (±6.43)
44	N	H, H	NH_2	75.0 (±18.08)
45	N	Me, Me	NH_2	107.7 (±25.14)

Table 4. Olefin, diol and oxime analogues as ring-truncated deguelin

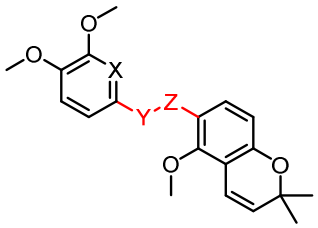

Code	X	Y, Z	WB (100 nM)
46	C-F	-CH=CH-	133.8 (±40.03)
47	N	-CH=CH-	133.2 (±24.03)
48	C-F	-CH(OH)-CH(OH)-	68.1 (±4.23)
49	N	-CH(OH)-CH(OH)-	68.9 (±1.46)
50a	N	-CH_2-C(=NOH)-	78.5 (±25.36)
50b	N	-CH_2-C(=NOH)-	79.2 (±34.62)
51	N	-CH_2-C(=$NOCH_3$)-	64.8 (±19.78)

Table 5. HIF-1α inhibition of the selected potent compounds

	WB (10 nM)	WB (100 nM)
Deguelin	94.0	64
16*S*	88.4 (±11.53)	44.2 (±33.24)
25	63.2 (±17.53)	52.2 (±12.56)
33	81.6 (±22.07)	35.0 (±6.05)
38	80.9 (±12.67)	48.8 (±2.99)
40	93.6 (±10.89)	64.1 (±20.46)
51	74.0 (±4.75)	64.8 (±19.78)

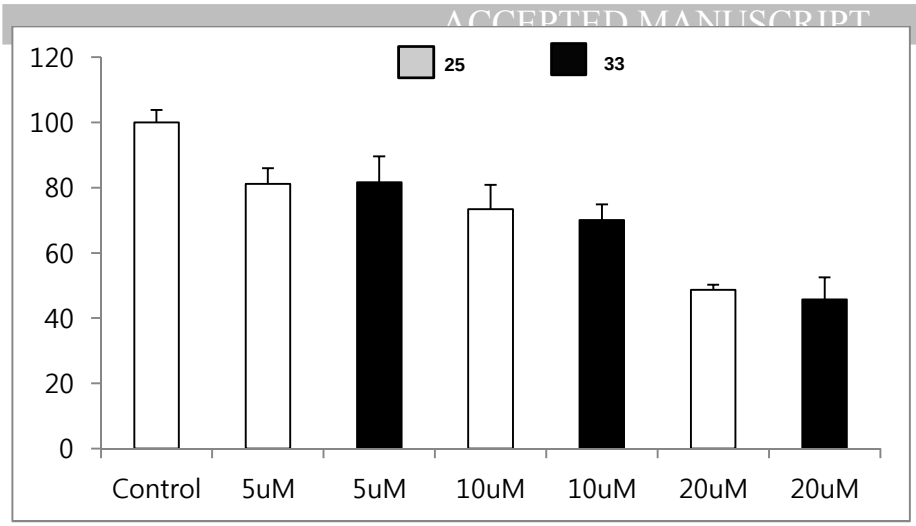

Figure 3. Antitumor activity of **25** and **33** in H1299

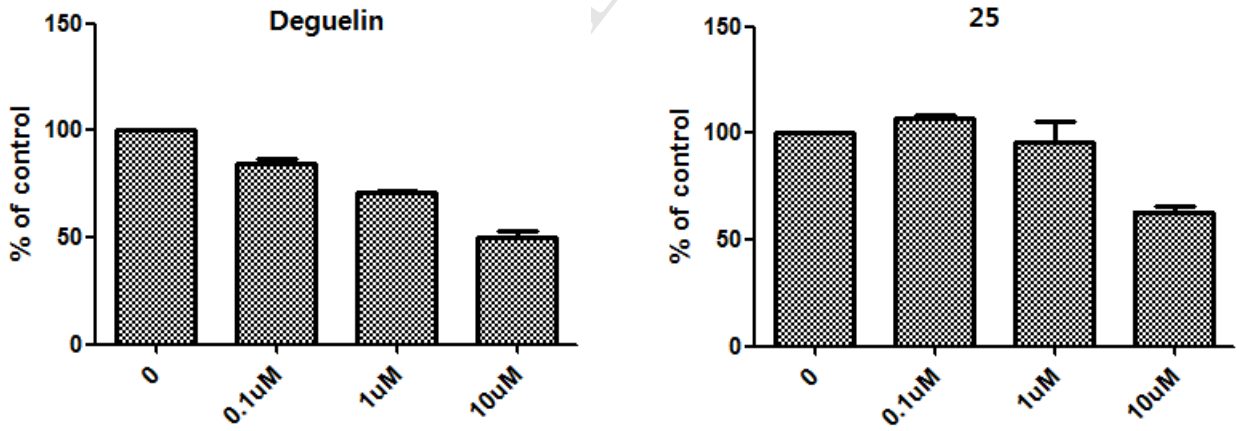

Figure 4. Effect of deguelin and **25** on the viability of mouse hippcampus (HT-22)

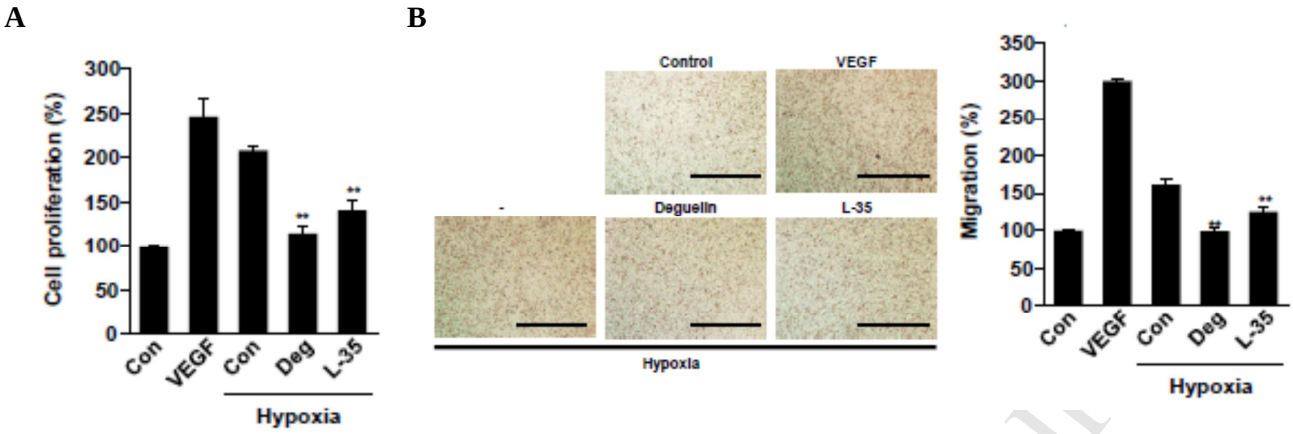

Figure 5. Anti-angiogenesis activity of **25** in HRMECs (A: proliferation assay; B: migration assay)

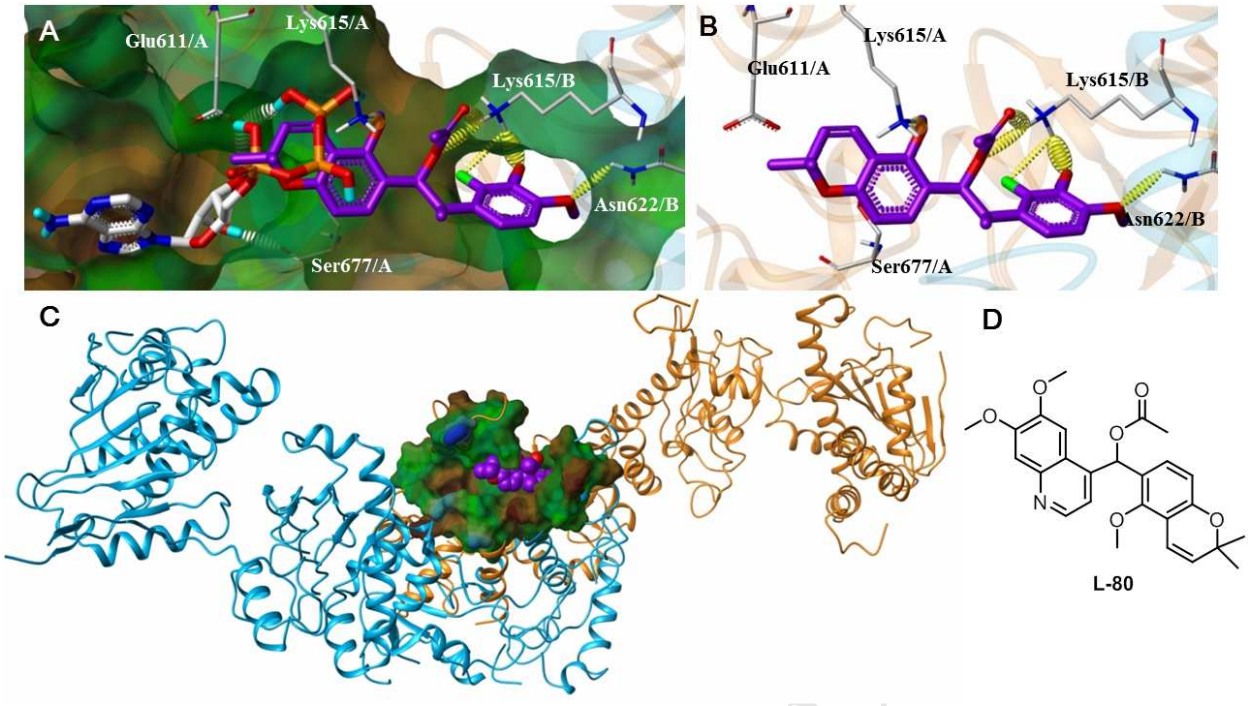

Figure 6. Molecular modeling of **25**
(A) Overlay of the docking pose of **25** (purple carbon) and ATP (white carbon) in the active site of the hHsp90 C-terminal. The key amino acid residues of the binding site are represented by the grey carbon capped stick. The active site is shown as a lipophilicity property surface map (brown colour: hydrophobic; blue colour: hydrophilic) (B) Docked pose of **25**. The dashed ellipsoids are hydrogen-bonding interactions (<2.8 Å). A and B indicate the chain names. (C) Binding site for **25** in the dimerization interface of the open state hHsp90. **25** is represented by the purple CPK model. Chain A is shown as an orange ribbon, and chain B is a cyan ribbon. (D) Structure of L-80

- A series of ring-truncated deguelin analogs were designed and synthesized as HIF-1α inhibitors.
- Compounds **25** and **33** exhibited potent HIF-1α inhibitions.
- Compound **25** showed significant antitumor and anti-angiogenic activities.

Supporting Information

Ring-truncated Deguelin Derivatives as Hypoxia Inducible Factor-1α (HIF-1α) Inhibitors

Ho Shin Kim, Mannkyu Hong, Su-Chan Lee, Ho-Young Lee, Young-Ger Suh, Dong-Chan Oh, Ji Hae Seo, Hoon Choi, Jun Yong Kim, Kyu-Won Kim, Jeong Hun Kim, Joohwan Kim, Young-Myeong Kim, So-Jung Park, Hyun-Ju Park, and Jeewoo Lee*

Experimental

1. General

All chemical reagents were commercially available. Melting points were determined on a melting point Buchi B-540 apparatus. Silica gel column chromatography was performed on Silica Gel 60, 230–400 mesh, Merck. Proton NMR spectra were recorded on a JEOL JNM-LA 300 at 300 MHz and Bruker Analytik, DE/AVANCE Digital 400 at 400 MHz or Bruker AMX-500 (500 MHz) spectrometer. Chemical shifts are reported in ppm units with tetramethylsilane as a reference standard. Optical rotations were measured using JASCO DIP-1000 digital polarimeter at ambient temperature using a 100 mm cell of 2 mL capacity. Mass spectra and HRMS results were recorded on VG Trio-2 GC−MS instrument and JEOL JMS-AX instrument, respectively.

2. General procedure

2.1. Carbon-Carbon bond formation (Procedure A)

To a solution of phenylsulfonyl compound (1.0 equiv) in THF was added dropwise 2.5M n-BuLi solution in n-hexane (1.5 equiv) at −78 °C. The reaction mixture was stirred for 20 min at −78 °C, and aldehyde (1.0 equiv) was added. The reaction mixture was stirred for an additional 30 min and was warmed to ambient temperature. The reaction mixture was quenched with saturated NH_4Cl solution and extracted with EtOAc. The organic layer was washed with brine, dried over $MgSO_4$, and concentrated under reduced pressure. The residue was purified by flash column

chromatography on silica gel to afford the corresponding alcohol. Diastereomer was not separated completely and directly oxidized to ketone.

2.2. DMP oxidation (Procedure B)

To a solution of alcohol in DCM was added Dess−Martin periodinane (1.0 equiv). After being stirred for 1 h, the reaction mixture was diluted with DCM and neutralized with saturated $NaHCO_3$ solution, dried over $MgSO_4$, and concentrated under reduced pressure. The residue was purified by flash column chromatography on silica gel to afford the corresponding oxidized product.

2.3. Desulfonylation (Procedure C)

To a solution of ketone (1.0 equiv) in dry benzene, $(n\text{-}Bu)_3SnH$ (2.0 equiv) and AIBN (0.1 equiv) were added. The reaction mixture was refluxed for 2 h and then cooled to room temperature. It was quenched with water and extracted with EtOAc, washed with brine several times, dried over $MgSO_4$, and concentrated under reduced pressure. The residue was purified by flash column chromatography on silica gel (including 10 % potassium fluoride to remove the residue of tin compound) to afford the corresponding desulfonylated product.

2.4. Alkylation (Procedure D)

To a solution of ketone in DMF was added NaH (1.0 – 2.0 equiv) at 0 ^oC. After being stirred for 30 min, alkylhalide (1.0 – 2.0 equiv) was added dropwise at 0 ^oC. The reaction mixture was stirred for an additional 1 h and warmed to room temperature. The reaction mixture was quenched with water and extracted with EtOAc, washed with brine several times, dried over $MgSO_4$, and concentrated under reduced pressure. The residue was purified by flash column chromatography on silica gel to afford the corresponding alkylated product.

2.5. Reduction (Procedure E)

To a solution of ketone in MeOH was added $NaBH_4$ (1.0–10.0 equiv) at 0 ^oC. The reaction mixture was stirred for 30 min and quenched with H_2O. The mixture was extracted with EtOAc, and the organic layer was washed with brine, dried over $MgSO_4$, and concentrated under reduced pressure. The residue was purified by flash columnchromatography on silica gel to afford the corresponding alcohol product.

2.6. Acylation (Procedure F)

To a solution of alcohol in DCM, pyridine (1.0 equiv) and acyl chloride (1.0 equiv) were added dropwise at 0 ^{o}C. After being stirred for 1 h, the reaction mixture was diluted with DCM and neutralized with saturated $NaHCO_3$ solution, dried over $MgSO_4$, and concentrated under reduced pressure. The residue was purified by flash column chromatography on silica gel to afford the corresponding acyl product.

2.7. Carbamoylation (Procedure G)

To a solution of alcohol in DCM, CDI (3.0 equiv) was added at 0 ^{o}C. After being stirred for 30 min, excess amount of ammonia or methylamine or dimethlyamine solution was added at 0 ^{o}C. The reaction mixture was heated to 40 ^{o}C and stirred for overnight. Then the mixture was evaporated to remove excess amount of ammonia and then extracted with DCM, dried over $MgSO_4$, and concentrated under reduced pressure. The residue was purified by flash column chromatography on silica gel to afford the corresponding carbamate product.

2.8. Phenylsulfonylation (Procedure H)

To a solution of alcohol in MC was added $SOCl_2$ (1.5 equiv) dropwise at 0 ^{o}C. After being stirred for 30 min, the mixture was evaporated to remove excess amount of $SOCl_2$ and directly used for the next step. $NaSO_2Ph$ was added to the crude compound in DMF at 0 ^{o}C and the mixture was warmed to room temperature. After being stirred for overnight, the mixture was extracted with EtOAc, dried over $MgSO_4$, and concentrated under reduced pressure. The residue was purified by flash column chromatography on silica gel to afford the corresponding phenylsulfonyl product.

2.9. Elimination (Procedure I)

To a solution of alcohol (1.0 equiv) in toluene, p-toluene sulfonic acid was added (1.5 equiv) and reflux for 1 h. Then it was cooled to the room temperature, neutralized with $NaHCO_3$, extracted with EtOAc, washed by water several times, dried over $MgSO_4$ and concentrated under reduced pressure. The residue was purified by flash column chromatography on silica gel to afford the corresponding trans-olefin product.

2.10. Diolation (Procedure J)

The olefin compound was dissolved in the solution of acetone and water (1:1). NMO (1.1 equiv) and OsO_4 (0.01 equiv) was added slowly at 0 ^oC. The reaction mixture was stirred for 5 min. Then the mixture was extracted with EtOAc, washed by water several times, dried over $MgSO_4$ and concentrated under reduced pressure. The residue was purified by flash column chromatography on silica gel to afford the corresponding syn diol product.

2.11. Oximation (Procedure K)

To a solution of ketone (1.0 equiv) in EtOH and water (1:1), hydroxylamine (or methoxyamine) hydrochloride (2.0 equiv) and sodium acetate (3.0 equiv) was added. The reaction mixture was refluxed for 2 h and then cooled to room temperature. Then the mixture was extracted with EtOAc, washed by water several times, dried over $MgSO_4$ and concentrated under reduced pressure. The residue was purified by flash column chromatography on silica gel to afford the corresponding oxime or methyl oxime product.

3. Chemical Spectra

3.1. (2-Fluoro-3,4-dimethoxyphenyl)methanol (5).

Alcohol compound **5** was synthesized through reduction of aldehyde **3** by procedure E, 90% yield; ^{1}H-NMR ($CDCl_3$, 300MHz) δ 7.04 (m, 1H), 6.67 (d, 1H, *J* = 8.4 Hz), 4.68 (d, 1H, *J* = 4.6 Hz), 3.93 (s, 3H), 3.87 (s, 3H)

3.2. (5,6-Dimethoxypyridin-2-yl)methanol (6).

Alcohol compound **6** was synthesized through reduction of aldehyde **4** by procedure E, 95% yield; ^{1}H-NMR ($CDCl_3$, 300MHz) δ 7.04 (d, 1H, *J* = 7.7 Hz), 6.78 (d, 1H, *J* = 7.9 Hz), 4.61 (d, 1H, *J* = 5.3 Hz), 4.03 (s, 3H), 3.88 (s, 3H), 3.02 (t, 1H, *J* = 5.3 Hz)

3.3. 2-Fluoro-3,4-dimethoxy-1-((phenylsulfonyl)methyl)benzene (7).

Compound **7** was synthesized from **5** following procedure H, 75% yield; ^{1}H-NMR ($CDCl_3$, 300MHz) δ 7.66 (m, 3H), 7.47 (m, 2H), 7.04 (m, 1H), 6.68 (dd, 1H, *J* = 8.6, 1.7 Hz), 4.33 (s, 2H), 3.88 (s, 3H), 3.71 (d, 3H, *J* = 0.9 Hz)

3.4. 2,3-Dimethoxy-6-((phenylsulfonyl)methyl)pyridine (8).

Compound **8** was synthesized from **6** following procedure H, 75% yield; ^{1}H-NMR ($CDCl_3$, 300MHz) δ 7.68 (m, 3H), 7.45 (m, 2H), 6.99 (m, 2H), 4.40 (s, 2H), 3.86 (s, 3H), 3.51 (d, 3H, *J* = 0.9 Hz)

3.5. 2-(2-Fluoro-3,4-dimethoxyphenyl)-1-(5-methoxy-2,2-dimethyl-2H-chromen-6-yl)ethan-1-one (12).

Compound **12** was synthesized from compound **7** and **9** following procedure A, B and C, 90% yield, pale yellow oil; ^{1}H-NMR ($CDCl_3$, 300MHz) δ 7.57 (d, 1H, *J* = 8.6 Hz), 6.87 (m, 1H), 6.67 (dd, 1H, *J* = 8.6, 1.7 Hz), 6.65 (s, 1H), 6.60 (d, 1H, *J* = 1.5 Hz), 5.68 (d, 1H, *J* = 10.1 Hz), 4.25 (d, 1H, *J* = 0.9 Hz), 3.92 (d, 3H, *J* = 0.9 Hz), 3.86 (s, 3H), 3.84 (s, 3H), 1.46 (s, 1H); HRMS (FAB) calcd for $C_{22}H_{24}FO_5$ ($M + H^+$): 387.1608. Found: 387.1604.

3.6. 2-(5,6-Dimethoxypyridin-2-yl)-1-(5-methoxy-2,2-dimethyl-2H-chromen-6-yl)ethan-1-one (13).

Compound **13** was synthesized from compound **8** and **9** following procedure A, B and C, 90% yield, pale yellow oil; ^{1}H-NMR ($CDCl_3$, 300MHz) δ 7.62 (d, 1H, *J* = 8.6 Hz), 6.99 (d, 1H, *J* = 7.7 Hz), 6.79 (d, 1H, *J* = 7.9 Hz), 6.61 (d, 1H, *J* = 10.1 Hz), 6.58 (d, 1H, *J* = 8.6 Hz), 5.67 (d, 1H, *J* = 10.1 Hz), 4.29 (s, 1H), 3.91 (s, 3H), 3.84 (s, 3H), 3.82 (s, 3H), 1.45 (s, 6H); HRMS (FAB) calcd for $C_{21}H_{24}NO_5$ ($M + H^+$): 370.1654. Found: 370.1656.

3.7. 2-(2-Fluoro-3,4-dimethoxyphenyl)-1-(5-methoxy-2,2-dimethyl-2H-chromen-6-yl)propan-1-one (14).

Compound **14** was synthesized from compound **12** through methylation following procedure D, 40% yield, pale yellow oil; ^{1}H-NMR ($CDCl_3$, 300MHz) δ 7.43 (d, 1H, *J* = 8.6 Hz), 6.89 (m, 1H), 6.61 (dd, 1H, *J* = 8.8, 1.7 Hz), 6.60 (s, 1H), 6.55 (d, 1H, *J* = 2.0 Hz), 6.53 (d, 1H, *J* = 0.5 Hz), 5.64 (d, 1H. *J* = 10.1 Hz), 4.90 (q, 1H, *J* = 7.0 Hz), 3.88 (d, 3H, *J* = 0.9 Hz), 3.83 (s, 3H), 3.74 (s, 3H), 1.45 (d, 1H, *J* = 7.0 Hz), 1.43 (s, 3H), 1.40 (s, 3H); HRMS (FAB) calcd for $C_{23}H_{26}FO_5$ ($M + H^+$): 401.1764. Found: 401.1770.

3.8. 2-(2-Fluoro-3,4-dimethoxyphenyl)-1-(5-methoxy-2,2-dimethyl-2H-chromen-6-yl)-2-methylpropan-1-one (15).

Compound **15** was synthesized from compound **12** through dimethylation following procedure D, 45% yield, pale yellow oil; ^{1}H-NMR ($CDCl_3$, 300MHz) δ 7.00 (m, 1H), 6.77 (d, 1H, *J* = 9.2 Hz), 6.68 (dd, 1H, *J* = 8.8, 1.7 Hz), 6.54 (d, 1H, *J* = 9.9 Hz), 6.32 (d, 1H, *J* = 9.2 Hz), 5.63 (d, 1H. *J* = 9.9 Hz), 3.87 (s, 3H), 3.82 (d, 3H, *J* = 0.9 Hz), 3.79 (s, 3H), 1.58 (s, 6H), 1.40 (s, 6H); HRMS (FAB) calcd for $C_{24}H_{28}FO_5$ ($M + H^+$): 415.1921. Found: 415.1915.

3.9. 2-(5,6-Dimethoxypyridin-2-yl)-1-(5-methoxy-2,2-dimethyl-2H-chromen-6-yl)propan-1-one (16).

Compound **16** was synthesized from compound **13** through methylation following procedure D, 40% yield, pale yellow oil; ^{1}H-NMR ($CDCl_3$, 300MHz) δ 7.46 (d, 1H, *J* = 8.6 Hz), 6.94 (d, 1H, *J* = 7.9 Hz), 6.77 (d, 1H, *J* = 7.9 Hz), 6.58 (d, 1H, *J* = 10.1 Hz), 6.52 (dd, 1H, *J* = 8.4, 0.6 Hz), 5.64 (d, 1H, *J* = 10.1 Hz), 4.74 (q, 1H, *J* = 7.0 Hz), 3.91 (s, 3H), 3.81 (s, 3H), 3.75 (s, 3H), 1.51 (d, 1H, *J* = 7.0 Hz), 1.42 (s, 3H), 1.41 (s, 3H); HRMS (FAB) calcd for $C_{22}H_{26}NO_5$ ($M + H^+$): 384.1811. Found: 384.1808.

3.10. 2-(5,6-Dimethoxypyridin-2-yl)-1-(5-methoxy-2,2-dimethyl-2H-chromen-6-yl)-2-methylpropan-1-one (17).

Compound **17** was synthesized from compound **13** through dimethylation following procedure D, 43% yield, pale yellow oil; ^{1}H-NMR ($CDCl_3$, 300MHz) δ 7.00 (d, 1H, *J* = 7.9 Hz), 6.85 (d, 1H, *J* = 8.1 Hz), 6.54 (d, 1H, *J* = 9.9 Hz), 6.34 (d, 1H, *J* = 8.6 Hz), 6.26 (d, 1H, *J* = 8.4 Hz), 5.63 (d, 1H, *J* = 9.9 Hz), 3.94 (s, 3H), 3.87 (s, 3H), 3.76 (s, 3H), 1.57 (s, 6H), 1.40 (s, 6H); HRMS (FAB) calcd for $C_{23}H_{28}NO_5$ ($M + H^+$): 398.1967. Found: 398.1968.

3.11. 2-(2-Fluoro-3,4-dimethoxyphenyl)-1-(5-methoxy-2,2-dimethyl-2H-chromen-6-yl)ethan-1-ol (18).

Compound **18** was synthesized from compound **12** through reduction following procedure E, 90% yield, pale yellow oil; ^{1}H-NMR ($CDCl_3$, 300MHz) δ 7.16 (d, 1H, *J* = 8.4 Hz), 6.88 (m, 1H), 6.58 (m, 3H), 5.65 (d, 1H, *J* = 9.9 Hz), 6.32 (d, 1H, *J* = 9.2 Hz), 5.63 (d, 1H. *J* = 9.9 Hz), 5.12 (dd, 1H, *J* = 8.6, 4.4Hz), 3.90 (s, 3H), 3.86 (s, 3H), 3.78 (s, 3H), 3.00 (m, 2H), 1.44 (s, 3H), 1.42 (s, 3H); HRMS (FAB) calcd for $C_{22}H_{24}FO_4$ ($M - H_2O + H^+$): 371.1659. Found: 371.1659.

3.12. 2-(2-Fluoro-3,4-dimethoxyphenyl)-1-(5-methoxy-2,2-dimethyl-2H-chromen-6-yl)propan-1-ol (19).

Compound **19** was synthesized from compound **14** through reduction following procedure E, major 80%, minor compound 4% yield, pale yellow oil; ^{1}H-NMR ($CDCl_3$, 300MHz) δ 7.08 (d, 1H, *J* = 8.4 Hz), 7.01 (d, 1H, *J* = 7.9 Hz), 6.73 (dd, 1H, *J* = 8.6, 2.5 Hz), 6.59 (m. 2H), 5.65 (d, 1H, *J* = 9.6 Hz), 4.97 (d, 1H, *J* = 6.6 Hz), 3.90 (d, 3H, *J* = 0.8 Hz), 3.87 (s, 3H), 3.83 (s, 3H), 3.39 (p, 1H, *J* = 7.14 Hz), 1.96 (m. 1H), 1.44 (s, 3H), 1.42 (s, 3H), 1.10 (d, 3H, *J* = 7.14 Hz); HRMS (FAB) calcd for $C_{23}H_{28}FO_5$ ($M + H^+$): 403.1921. Found: 403.1933.

3.13. 2-(2-Fluoro-3,4-dimethoxyphenyl)-1-(5-methoxy-2,2-dimethyl-2H-chromen-6-yl)-2-methylpropan-1-ol (20).

Compound **20** was synthesized from compound **15** through reduction following procedure E, 90% yield, pale yellow oil; ^{1}H-NMR ($CDCl_3$, 300MHz) δ 7.10 (d, 1H, *J* = 8.6 Hz), 6.94 (m, 1H), 6.59 (m, 3H), 5.63 (d, 1H, *J* = 9.9 Hz), 5.44 (s, 1H), 3.94 (s, 3H), 3.87 (s, 3H), 3.76 (s, 3H), 1.45 (s, 3H), 1.39 (s, 3H), 1.33 (s, 3H), 1.25 (s, 3H); HRMS (FAB) calcd for $C_{24}H_{28}FO_4$ ($M–H_2O + H^+$) : 399.1972. Found: 399.1978.

3.14. 2-(5,6-Dimethoxypyridin-2-yl)-1-(5-methoxy-2,2-dimethyl-2H-chromen-6-yl)ethan-1-ol (21).

Compound **21** was synthesized from compound **13** through reduction following procedure E, 90% yield, pale yellow oil; ^{1}H-NMR ($CDCl_3$, 300MHz) δ 7.25 (d, 1H, *J* = 8.6 Hz), 6.99 (d, 1H, *J* = 7.9 Hz), 6.65 (d, 1H, *J* = 7.7 Hz), 6.59 (d, 1H, *J* = 8.1 Hz), 6.57 (d, 1H, *J* = 9.9 Hz), 5.64 (d, 1H, *J* = 9.9 Hz), 5.38 (br-s, 1H), 5.29 (t, 1H, *J* = 5.9 Hz), 4.04 (s, 2H), 3.87 (s, 3H), 3.78 (s, 2H), 2.98 (d, 2H, *J* = 5.9 Hz), 1.44 (s, 3H), 1.41 (s, 3H); HRMS (FAB) calcd for $C_{21}H_{26}NO_5$ ($M + H^+$): 372.1811. Found: 372.1807.

3.15. 2-(5,6-Dimethoxypyridin-2-yl)-1-(5-methoxy-2,2-dimethyl-2H-chromen-6-yl)propan-1-ol (22).

Compound **22** was synthesized from compound **16** through reduction following procedure E, 90% yield, pale yellow oil; ^{1}H-NMR ($CDCl_3$, 300MHz) δ 6.92 (d, 1H, *J* = 7.9 Hz), 6.85 (d, 1H, *J* = 8.4 Hz), 6.57 (d, 1H, *J* = 9.9 Hz), 6.53 (d, 1H, *J* = 7.9 Hz), 6.46 (d, 1H, *J* = 8.6 Hz), 5.63 (d, 1H, *J* = 9.9

Hz), 5.08 (d, 1H, *J* = 5.5 Hz), 4.05 (s, 3H), 3.80 (s, 2H), 3.73 (s, 3H), 3.09 (p, 1H, *J* = 7.0 Hz), 1.47 (s, 3H), 1.37 (s, 3H), 1.31 (d, 3H, *J* = 7.1 Hz); HRMS (FAB) calcd for $C_{22}H_{28}NO_5$ ($M + H^+$): 386.1967. Found: 386.1964.

3.16. 2-(5,6-Dimethoxypyridin-2-yl)-1-(5-methoxy-2,2-dimethyl-2H-chromen-6-yl)-2-methylpropan-1-ol (23).

Compound **23** was synthesized from compound **17** through reduction following procedure E, 90% yield, pale yellow oil; ^{1}H-NMR ($CDCl_3$, 300MHz) δ 6.99 (d, 1H, *J* = 8.0 Hz), 6.67 (d, 1H, *J* = 8.1 Hz), 6.56 (d, 1H, *J* = 9.9 Hz), 6.43 (d, 1H, *J* = 8.4 Hz), 6.37 (d, 1H, *J* = 8.4 Hz), 6.27 (d, 1H, *J* = 5.9 Hz), 5.61 (d, 1H, *J* = 9.9 Hz), 5.05 (d, 1H, *J* = 5.9 Hz), 4.08 (s, 3H), 3.88 (s, 3H), 3.74 (s, 3H), 1.44 (s, 3H), 1.43 (s, 3H), 1.35 (s, 3H), 1.18 (s, 3H); HRMS (FAB) calcd for $C_{23}H_{30}NO_5$ ($M + H^+$): 400.2124. Found: 400.2125.

3.17. 2-(2-Fluoro-3,4-dimethoxyphenyl)-1-(5-methoxy-2,2-dimethyl-2H-chromen-6-yl)ethyl acetate (24).

Compound **24** was synthesized from compound **18** through acetylation following procedure F, 70% yield, white solid, mp = 91-92 ^{o}C; ^{1}H-NMR ($CDCl_3$, 300MHz) δ 7.02 (d, 1H, *J* = 8.7 Hz), 6.73 (m, 1H), 6.53 (m, 3H), 6.19 (m, 1H), 5.61 (d, 1H, *J* = 10.2 Hz), 3.88 (d, 3H, *J* = 0.9 Hz), 3.82 (s, 3H), 3.76 (s, 3H), 3.02 (m, 2H), 1.98 (s, 3H). 1.42 (s, 3H), 1.37 (s, 3H); HRMS (FAB) calcd for $C_{24}H_{28}FO_6$ ($M + H^+$): 431.1870. Found: 431.1875.

3.18. (*rel*-1*R*,2*S*)-2-(2-Fluoro-3,4-dimethoxyphenyl)-1-(5-methoxy-2,2-dimethyl-2H-chromen-6-yl)propyl acetate (25).

Compound **25** was synthesized from compound **19** through acetylation following procedure F, 70% yield, pale yellow oil; ^{1}H-NMR ($CDCl_3$, 300MHz) δ 7.01 (d, 1H, *J* = 8.4 Hz), 6.95 (d, 1H, *J* = 7.9 Hz), 6.67 (dd, 1H, *J* = 8.8, 1.7 Hz), 6.58 (d, 1H, *J* = 9.9 Hz), 6.56 (d, 1H, *J* = 8.4 Hz), 6.15 (d, 1H, *J* = 9.2 Hz), 5.62 (d, 1H, *J* = 6.2 Hz), 3.88 (s, 6H), 3.85 (s, 3H), 3.50 (p, 1H, *J* = 7.3 Hz), 1.85 (s, 3H). 1.45 (s, 3H), 1.40 (s, 3H), 1.11 (d, 1H, *J* = 7.1 Hz); HRMS (FAB) calcd for $C_{25}H_{30}FO_6$ ($M + H^+$): 445.2026. Found: 445.2019.

3.19. (*rel*-1S,2S)-2-(2-Fluoro-3,4-dimethoxyphenyl)-1-(5-methoxy-2,2-dimethyl-2H-chromen-6-yl)propyl acetate (26).

Compound **26** was synthesized from compound **19** minor through acetylation general procedure F, 45% yield, pale yellow oil; ^{1}H-NMR ($CDCl_3$, 300MHz) δ 6.91 (d, 1H, *J* = 8.4 Hz), 6.75 (m, 1H), 6.52 (m, 2H), 6.48 (s, 1H), 6.21 (d, 1H, *J* = 6.6 Hz), 5.59 (d, 1H, *J* = 9.9 Hz), 3.85 (s, 3H), 3.82 (s, 3H), 3.77 (s, 3H), 3.59 (p, 1H, *J* = 6.8 Hz), 2.05 (s, 3H). 1.41 (s, 3H), 1.37 (s, 3H), 1.26 (d, 1H, *J* = 6.9 Hz); HRMS (FAB) calcd for $C_{25}H_{29}FO_6$ (M^+): 444.1958. Found: 444.1948.

3.20. 2-(2-Fluoro-3,4-dimethoxyphenyl)-1-(5-methoxy-2,2-dimethyl-2H-chromen-6-yl)-2-methylpropyl acetate (27).

Compound **27** was synthesized from compound **20** through acetylation following procedure F, 40% yield, white solid, mp = 101-102 ^{o}C; ^{1}H-NMR ($CDCl_3$, 300MHz) δ 6.91 (d, 1H, *J* = 12.5 Hz), 6.82 (m, 1H), 6.56 (dd, 1H, *J* = 9.0, 1.7 Hz), 6.55 (s, 1H), 6.52 (m, 1H), 5.60 (d, 1H, *J* = 9.9 Hz), 3.92 (s, 3H), 3.85 (s, 6H), 1.90 (s, 3H), 1.46 (s, 3H), 1.37 (s, 3H), 1.32 (s, 3H); HRMS (FAB) calcd for $C_{26}H_{31}FO_6$ (M^+): 458.2105. Found: 458.2108.

3.21. (1-(2-Fluoro-3,4-dimethoxyphenyl)cyclopropyl)-1-(5-methoxy-2,2-dimethyl-2H-chromen-6-yl)methyl acetate (28).

Compound **28** was synthesized from compound **12** through alkyation using dibromoethane and acetylation following procedure D and F, 35% yield, white solid, mp = 48-49 ^{o}C; ^{1}H-NMR ($CDCl_3$, 300MHz) δ 6.74 (m, 1H), 6.57 (d, 1H, *J* = 9.9 Hz), 6.54 (d, 1H, *J* = 8.4 Hz), 6.51 (d, 1H, *J* = 8.6 Hz), 6.37 (d, 1H, *J* = 8.4 Hz), 5.90 (s, 1H), 5.63 (d, 1H, *J* = 9.9 Hz), 3.84 (s, 6H), 3.81 (s, 3H), 2.05 (s, 3H), 1.44 (s, 3H), 1.37 (s, 3H), 1.19 (m, 1H), 0.98 (m, 1H), 0.83 (m, 1H), 0.74 (m, 1H); HRMS (FAB) calcd for $C_{26}H_{29}FO_6$ (M^+): 456.1948. Found: 456.1952.

3.22. 2-(2-Fluoro-3,4-dimethoxyphenyl)-1-(5-methoxy-2,2-dimethyl-2H-chromen-6-yl)ethyl propionate (29).

Compound **29** was synthesized from compound **18** through propionylation following procedure F, 70% yield, pale yellow oil; ^{1}H-NMR ($CDCl_3$, 300MHz) δ 7.03 (d, 1H, *J* = 8.3 Hz), 6.75 (m, 1H), 6.57 (dd, 1H, *J* = 8.6, 1.7 Hz), 6.55 (d, 1H, *J* = 9.2 Hz), 6.22 (m, 1H), 5.63 (d, 1H, *J* = 9.9 Hz), 3.88 (s, 3H). 3.84 (s, 3H), 3.80 (s, 3H), 3.04 (d, 2H, *J* = 6.0 Hz), 2.28 (d, 2H, *J* = 7.5 Hz), 1.44 (s, 3H), 1.40 (s, 3H), 1.06 (t, 3H, *J* = 7.5 Hz); HRMS (FAB) calcd for $C_{25}H_{30}FO_6$ ($M + H^+$): 445.2026. Found: 445.2033.

3.23. 2-(2-Fluoro-3,4-dimethoxyphenyl)-1-(5-methoxy-2,2-dimethyl-2H-chromen-6-yl)propyl propionate (30).

Compound **30** was synthesized from compound **19** through acetylation following procedure F, 70% yield, pale yellow oil; ^{1}H-NMR ($CDCl_3$, 300MHz) δ 7.00 (d, 1H, *J* = 8.4 Hz), 6.98 (m, 1H), 6.65 (dd, 1H, *J* = 8.8, 1.8 Hz), 6.57 (d, 1H, *J* = 9.9 Hz), 6.54 (d, 1H, *J* = 8.6 Hz), 6.15 (d, 1H, *J* = 9.2 Hz), 5.61 (d, 1H, *J* = 9.9 Hz), 3.89 (s, 3H). 3.88 (s, 3H), 3.87 (s, 3H), 3.49 (p, 1H, *J* = 7.3 Hz), 2.12 (dq, 2H, *J* = 7.7, 1.7 Hz), 1.45 (s, 3H), 1.40 (s, 3H), 1.12 (d, 3H, *J* = 7.1 Hz), 0.94 (t, 3H, *J* = 7.5 Hz); HRMS (FAB) calcd for $C_{26}H_{31}FO_6$ (M^+): 458.2105. Found: 458.2096.

3.24. 2-(2-Fluoro-3,4-dimethoxyphenyl)-1-(5-methoxy-2,2-dimethyl-2H-chromen-6-yl)-2-methylpropyl propionate (31).

Compound **31** was synthesized from compound **20** through propionylation following procedure F, 70% yield, pale yellow oil; ^{1}H-NMR ($CDCl_3$, 300MHz) δ 6.87 (d, 1H, *J* = 8.4 Hz), 6.80 (m, 1H), 6.55 (dd, 1H, *J* = 10.1, 1.7 Hz), 6.53 (m, 3H), 5.59 (d, 1H, *J* = 9.9 Hz), 3.91 (s, 3H). 3.87 (s, 3H), 3.85 (s, 3H), 2.18 (q, 2H, *J* = 7.7 Hz), 1.42 (s, 3H), 1.37 (s, 3H), 1.32 (s, 3H), 0.96 (t, 3H, *J* = 7.5 Hz); HRMS (FAB) calcd for $C_{27}H_{34}FO_6$ ($M + H^+$): 473.2339. Found: 473.2343.

3.25. 2-(2-Fluoro-3,4-dimethoxyphenyl)-1-(5-methoxy-2,2-dimethyl-2H-chromen-6-yl)ethyl cyclopropanecarboxylate (32).

Compound **32** was synthesized from compound **18** through cyclopropane carbonylation following procedure F, 70% yield, pale yellow oil; ^{1}H-NMR ($CDCl_3$, 300MHz) δ 7.02 (d, 1H, *J* = 8.4 Hz), 6.76 (m, 1H), 6.57 (dd, 1H, *J* = 8.6, 1.7 Hz), 6.56 (m, 2H), 6.19 (m 1H), 5.63 (d, 1H, *J* = 9.9 Hz), 3.88 (d, 3H, *J* = 0.5 Hz), 3.84 (s, 3H), 3.78 (s, 3H), 3.05 (d, 2H, *J* = 6.2 Hz), 1.59 (m, 1H), 1.44 (s, 3H), 1.40 (s, 3H), 0.92 (m, 2H), 0.81 (m, 2H); HRMS (FAB) calcd for $C_{26}H_{30}FO_6$ ($M + H^+$): 457.2026. Found: 457.2033.

3.26. 2-(2-Fluoro-3,4-dimethoxyphenyl)-1-(5-methoxy-2,2-dimethyl-2H-chromen-6-yl)propyl cyclopropanecarboxylate (33).

Compound **33** was synthesized from compound **19** through cyclopropane carbonylation following procedure F, 70% yield, pale yellow oil; ^{1}H-NMR ($CDCl_3$, 300MHz) δ 6.98 (d, 1H, *J* = 8.4 Hz), 6.97 (m, 1H), 6.67 (dd, 1H, *J* = 8.6, 1.5 Hz), 6.57 (d, 1H, *J* = 9.5 Hz), 6.56 (d, 1H, *J* = 8.3 Hz), 6.11

(d, 1H, *J* = 9.0 Hz), 5.64 (d, 1H, *J* = 9.9 Hz), 3.88 (d, 3H, *J* = 0.5 Hz), 3.87 (s, 6H), 3.49 (p, 1H, *J* = 7.3 Hz), 1.45 (s, 3H), 1.43 (m, 1H), 1.40 (s, 3H), 1.11 (d, 3H, *J* = 7.1 Hz), 0.76 (m, 2H), 0.69 (m, 2H); HRMS (FAB) calcd for $C_{27}H_{31}FO_6$ (M^+): 470.2105. Found: 470.2115.

3.27. 2-(2-Fluoro-3,4-dimethoxyphenyl)-1-(5-methoxy-2,2-dimethyl-2H-chromen-6-yl)butyl cyclopropanecarboxylate (34).

Compound **34** was synthesized from compound **12** through alkyation using iodoethane and cyclopropane carbonylation following procedure D and F, 45% yield, white solid, mp = 50-51 ^oC; ^1H-NMR ($CDCl_3$, 300MHz) δ 6.95 (m, 1H), 6.88 (d, 1H, *J* = 8.4 Hz), 6.68 (dd, 1H, *J* = 8.8, 1.5 Hz), 6.57 (d, 1H, *J* = 10.1 Hz), 6.52 (d, 1H, *J* = 8.4 Hz), 6.18 (d, 1H, *J* = 8.4 Hz), 5.63 (d, 1H, *J* = 9.9 Hz), 3.88 (d, 6H, *J* = 0.5 Hz), 3.86 (s, 3H), 3.24 (m, 1H), 1.57 (m, 2H), 1.45 (s, 3H), 1.42 (m, 1H), 1.40 (s, 3H), 0.80 (m, 2H), 0.70 (t, 3H, *J* = 7.3 Hz), 0.65 (m, 2H); HRMS (FAB) calcd for $C_{28}H_{34}FO_6$ ($M + H^+$): 485.2339. Found: 485.2346.

3.28. 2-(2-Fluoro-3,4-dimethoxyphenyl)-1-(5-methoxy-2,2-dimethyl-2H-chromen-6-yl)-2-methylpropyl cyclopropanecarboxylate (35).

Compound **35** was synthesized from compound **20** through cyclopropane carbonylation following procedure F, 40% yield, white solid, mp = 58-59 ^oC; ^1H-NMR ($CDCl_3$, 300MHz) δ 6.89 (d, 1H, *J* = 10.8 Hz), 6.93 (m, 1H), 6.56 (dd, 1H, *J* = 9.0, 1.7 Hz), 6.51 (m, 3H), 5.60 (d, 1H, *J* = 10.1 Hz), 3.91 (s, 1H), 3.85 (s, 3H), 3.84 (s, 3H), 1.50 (m, 1H), 1.45 (s, 3H), 1.37 (s, 6H), 1.33 (s, 3H), 0.84 (m, 2H), 0.70 (m, 2H); HRMS (FAB) calcd for $C_{28}H_{34}FO_6$ ($M + H^+$): 485.2339. Found: 485.2344.

3.29. 2-(2-Fluoro-3,4-dimethoxyphenyl)-1-(5-methoxy-2,2-dimethyl-2H-chromen-6-yl)propyl cyclobutanecarboxylate (36).

Compound **36** was synthesized from compound **19** through cyclobutyl carbonylation following procedure F, 43% yield, pale yellow oil; ^1H-NMR ($CDCl_3$, 300MHz) δ 7.00 (d, 1H, *J* = 8.6 Hz), 6.96 (m, 1H), 6.68 (dd, 1H, *J* = 8.8, 1.7 Hz), 6.57 (m, 2H), 6.13 (d, 1H, *J* = 9.2 Hz), 5.64 (d, 1H, *J* = 9.9 Hz), 3.90 (s, 3H), 3.87 (s, 3H), 3.86 (s, 3H), 3.47 (p, 1H, *J* = 8.6 Hz), 2.93 (m, 1H), 2.05 (m, 2H), 1.97 (m, 2H), 1.95 (m, 2H), 1.45 (s, 3H), 1.40 (s, 3H), 1.11 (d, 3H, *J* = 7.1 Hz); HRMS (FAB) calcd for $C_{28}H_{34}FO_6$ ($M + H^+$): 485.2339. Found: 485.2346.

3.30. 2-(2-Fluoro-3,4-dimethoxyphenyl)-1-(5-methoxy-2,2-dimethyl-2H-chromen-6-yl)ethyl carbamate (37).

Compound **37** was synthesized from compound **18** through carbamoylation following procedure G, 42% yield, white solid, mp = 168-169 ^{o}C; ^{1}H-NMR ($CDCl_3$, 300MHz) δ 7.05 (d, 1H, *J* = 8.4 Hz), 6.77 (m, 1H), 6.58 (dd, 1H, *J* = 8.6, 1.7 Hz), 6.55 (m, 2H), 6.12 (m, 1H), 5.62 (d, 1H, *J* = 9.9 Hz), 4.53 (br-s, 2H), 3.88 (d, 3H, *J* = 0.8 Hz), 3.84 (s, 3H), 3.79 (s, 3H), 3.05 (m, 2H), 1.44 (s, 3H), 1.40 (s, 3H); HRMS (FAB) calcd for $C_{23}H_{26}FNO_6$ (M^+): 431.1744. Found: 431.1746.

3.31. 2-(2-Fluoro-3,4-dimethoxyphenyl)-1-(5-methoxy-2,2-dimethyl-2H-chromen-6-yl)propyl carbamate (38).

Compound **38** was synthesized from compound **19** through carbamoylation following procedure G, 35% yield, white solid, mp = 75-76 ^{o}C; ^{1}H-NMR ($CDCl_3$, 300MHz) δ 7.01 (d, 1H, *J* = 7.0 Hz), 7.00 (m, 1H), 6.67 (dd, 1H, *J* = 8.6, 1.7 Hz), 6.59 (d, 1H, *J* = 9.9 Hz), 6.56 (d, 1H, *J* = 8.4 Hz), 6.03 (d, 1H, *J* = 9.2 Hz), 5.65 (d, 1H, *J* = 9.9 Hz), 4.39 (bs, 2H), 3.89 (s, 3H), 3.88 (d, 3H, *J* = 0.7 Hz), 3.87 (s, 3H), 3.48 (p, 1H, *J* = 7.3 Hz), 1.45 (s, 3H), 1.40 (s, 3H), 1.09 (d, 3H, *J* = 7.1 Hz); HRMS (FAB) calcd for $C_{23}H_{26}FNO_6$ (M^+): 445.1901. Found: 445.1895.

3.32. 2-(2-Fluoro-3,4-dimethoxyphenyl)-1-(5-methoxy-2,2-dimethyl-2H-chromen-6-yl)propyl methylcarbamate (39).

Compound **39** was synthesized from compound **19** through N-methyl carbamoylation following procedure G, 36% yield, white solid, mp = 74-75 ^{o}C; ^{1}H-NMR ($CDCl_3$, 300MHz) δ 7.00 (m, 1H), 6.97 (d, 1H, *J* = 8.6 Hz), 6.67 (dd, 1H, *J* = 8.6, 1.5 Hz), 6.59 (d, 1H, *J* = 9.9 Hz), 6.56 (d, 1H, *J* = 8.6 Hz), 6.02 (d, 1H, *J* = 9.0 Hz), 5.64 (d, 1H, *J* = 9.9 Hz), 4.47 (br-s, 1H), 3.91 (s, 3H), 3.8 (s, 3H), 3.86 (s, 3H), 3.44 (p, 1H, *J* = 7.9 Hz), 2.63 (d, 3H, *J* = 4.8 Hz), 1.44 (s, 3H), 1.40 (s, 3H), 1.11 (d, 3H, *J* = 7.1 Hz); HRMS (FAB) calcd for $C_{25}H_{31}FNO_6$ ($M + H^+$): 460.2135. Found: 460.2129.

3.33. 2-(2-Fluoro-3,4-dimethoxyphenyl)-1-(5-methoxy-2,2-dimethyl-2H-chromen-6-yl)propyl dimethylcarbamate (40).

Compound **40** was synthesized from compound **19** through N-dimethyl carbamoylation following procedure G, 33% yield, white solid, mp = 55-56 ^{o}C; ^{1}H-NMR ($CDCl_3$, 400MHz) δ 6.97 (m, 1H), 6.91 (d, 1H, *J* = 8.4 Hz), 6.64 (d, 1H, *J* = 8.6 Hz), 6.56 (d, 1H, *J* = 9.9 Hz), 6.50 (d, 1H, *J* = 8.4 Hz),

5.93 (d, 1H, *J* = 8.7 Hz), 5.60 (d, 1H, *J* = 9.9 Hz), 3.89 (s, 3H), 3.84 (s, 3H), 3.83 (s, 3H), 3.46 (p, 1H, *J* = 7.8 Hz), 2.79 (s, 3H), 2.73 (s, 3H), 1.42 (s, 3H), 1.37 (s, 3H), 1.10 (d, 3H, *J* = 7.2 Hz); HRMS (FAB) calcd for $C_{26}H_{32}FNO_6$ (M^+): 473.2214. Found: 473.2217.

3.34. 2-(5,6-Dimethoxypyridin-2-yl)-1-(5-methoxy-2,2-dimethyl-2H-chromen-6-yl)ethyl acetate (41).

Compound **41** was synthesized from compound **21** through acetylation following procedure F, 65% yield, pale yellow oil; ^{1}H-NMR ($CDCl_3$, 300MHz) δ 7.11 (d, 1H, *J* = 8.4 Hz), 6.91 (d, 1H, *J* = 7.9 Hz), 6.62 (d, 1H, *J* = 7.7 Hz), 6.56 (d, 1H, *J* = 8.3 Hz), 6.54 (d, 1H, *J* = 9.9 Hz), 6.47 (m, 1H), 5.62 (d, 1H, *J* = 10.1 Hz), 3.96 (s, 3H), 3.83 (s, 3H), 3.79 (s, 3H), 3.11 (m, 2H), 1.98 (s, 3H), 1.43 (s, 3H), 1.41 (s, 3H); HRMS (FAB) calcd for $C_{23}H_{28}NO_6$ (M + H^+): 414.1917. Found: 414.1911.

3.35. 2-(5,6-Dimethoxypyridin-2-yl)-1-(5-methoxy-2,2-dimethyl-2H-chromen-6-yl)propyl acetate (42).

Compound **42** was synthesized from compound **22** through acetylation following procedure F, 55% yield, white solid, mp = 115-116 ^{o}C; ^{1}H-NMR ($CDCl_3$, 300MHz) δ 7.10 (d, 1H, *J* = 8.4 Hz), 6.96 (d, 1H, *J* = 7.9 Hz), 6.70 (d, 1H, *J* = 7.7 Hz), 6.60 (m, 2H), 6.38 (d, 1H, *J* = 9.9 Hz), 5.64 (d, 1H, *J* = 9.9 Hz), 4.02 (s, 3H), 3.90 (s, 3H), 3.86 (s, 3H), 3.20 (p, 1H, *J* = 7.1 Hz), 1.80 (s, 3H), 1.46 (s, 3H), 1.41 (s, 3H), 1.04(d, 3H, *J* = 7.1 Hz); HRMS (FAB) calcd for $C_{24}H_{30}NO_6$ (M + H^+): 428.2073. Found: 428.2071.

3.36. 2-(5,6-Dimethoxypyridin-2-yl)-1-(5-methoxy-2,2-dimethyl-2H-chromen-6-yl)-2-methylpropyl acetate (43).

Compound **43** was synthesized from compound **23** through acetylation following procedure F, 35% yield, white solid, mp = 120-121 ^{o}C; ^{1}H-NMR ($CDCl_3$, 300MHz) δ 6.95 (d, 1H, *J* = 7.9 Hz), 6.89 (d, 1H, *J* = 8.4 Hz), 6.79 (d, 1H, *J* = 8.1 Hz), 6.63 (br-s, 1H), 6.57 (d, 1H, *J* = 9.9 Hz), 6.51 (d, 1H, *J* = 8.4 Hz), 5.61 (d, 1H, *J* = 10.1 Hz), 4.01 (s, 3H), 3.89 (s, 3H), 3.86 (s, 3H), 1.84(s, 3H), 1.46 (s, 3H), 1.39 (s, 3H), 1.36 (s, 3H), 1.17 (s, 3H); HRMS (FAB) calcd for $C_{25}H_{32}NO_6$ (M + H^+): 442.2230. Found: 442.2236.

3.37. 2-(5,6-Dimethoxypyridin-2-yl)-1-(5-methoxy-2,2-dimethyl-2H-chromen-6-yl)ethyl carbamate (44).

Compound **44** was synthesized from compound **21** through carbamoylation following procedure G, 35% yield,white solid, mp = 99-100 ^{o}C; ^{1}H-NMR ($CDCl_3$, 300MHz) δ 7.12 (d, 1H, *J* = 8.4 Hz), 6.91 (d, 1H, *J* = 7.9 Hz), 6.64 (d, 1H, *J* = 7.9 Hz), 6.57 (d, 1H, *J* = 8.2 Hz), 6.54 (d, 1H, *J* = 9.9 Hz), 6.37 (m, 1H), 5.62 (d, 1H, *J* = 9.9 Hz), 4.53 (br-s, 2H), 3.96 (s, 3H), 3.83 (s, 3H), 3.79 (s, 3H), 3.12 (m, 2H), 1.47 (s, 3H), 1.41 (s, 3H); HRMS (FAB) calcd for $C_{22}H_{26}N_2O_6$ (M^+): 414.1791. Found: 414.1800.

3.38. 2-(5,6-Dimethoxypyridin-2-yl)-1-(5-methoxy-2,2-dimethyl-2H-chromen-6-yl)-2-methylpropyl carbamate (45).

Compound **45** was synthesized from compound **23** through carbamoylation following procedure G, 35% yield,white solid, mp = 90-91 ^{o}C; ^{1}H-NMR ($CDCl_3$, 300MHz) δ 6.96 (d, 1H, *J* = 8.0 Hz), 6.91 (d, 1H, *J* = 8.4 Hz), 6.79 (d, 1H, *J* = 7.9 Hz), 6.55 (m, 3H), 5.62 (d, 1H, *J* = 9.9 Hz), 4.37 (br-s, 2H), 4.01 (s, 3H), 3.89 (s, 3H), 3.86 (s, 3H), 1.46 (s, 3H), 1.39 (s, 3H), 1.35 (s, 3H), 1.17 (s, 3H); HRMS (FAB) calcd for $C_{24}H_{31}N_2O_6$ ($M + H^+$): 443.2182. Found: 443.2187.

3.39. (*E*)-6-(2-Fluoro-3,4-dimethoxystyryl)-5-methoxy-2,2-dimethyl-2H-chromene (46).

Compound **46** was synthesized from compound **18** through elimination following procedure I, 85% yield,white solid, mp = 121-122 ^{o}C; ^{1}H-NMR ($CDCl_3$, 300MHz) δ 7.41 (d, 1H, *J* = 8.6 Hz), 7.26 (m, 2H), 7.07 (d, 1H, *J* = 16.7 Hz), 6.70 (dd, 1H, *J* = 8.8, 1.5 Hz), 6.64 (d, 1H, *J* = 2.6 Hz), 6.62 (s, 1H), 5.65 (d, 1H, *J* = 9.9 Hz), 3.94 (s, 3H), 3.90 (s, 3H), 3.78 (s, 3H), 1.44 (s, 6H); HRMS (FAB) calcd for $C_{22}H_{23}FO_4$ (M^+): 370.1580. Found: 370.1580.

3.40. (*E*)-2,3-Dimethoxy-6-(2-(5-methoxy-2,2-dimethyl-2H-chromen-6-yl)vinyl)pyridine (47).

Compound **47** was synthesized from compound **21** through elimination following procedure I, 88% yield,white solid, mp = 116-117 ^{o}C; ^{1}H-NMR ($CDCl_3$, 300MHz) δ 7.69 (d, 1H, *J* = 15.9 Hz), 7.41 (d, 1H, *J* = 8.6 Hz), 6.99 (d, 1H, *J* = 7.9 Hz), 6.97 (d, 1H, *J* = 15.9 Hz), 6.84 (d, 1H, *J* = 7.9 Hz), 6.64 (d, 1H, *J* = 10.1 Hz), 6.61 (d, 1H, *J* = 8.6 Hz), 5.65 (d, 1H, *J* = 9.9 Hz), 4.10 (s, 3H), 3.89 (s, 3H), 3.81 (s, 3H), 1.45 (s, 6H); HRMS (FAB) calcd for $C_{21}H_{23}NO_4$ (M^+): 353.1627. Found: 353.1629.

3.41. (*rel*-1S,2S)-1-(2-Fluoro-3,4-dimethoxyphenyl)-2-(5-methoxy-2,2-dimethyl-2H-chromen-6-yl)ethane-1,2-diol (48).

Compound **48** was synthesized from compound **46** through diolation following procedure J, 42% yield, white solid, mp = 69-70 ^{o}C; ^{1}H-NMR ($CDCl_3$, 400MHz) δ 7.14 (m, 1H), 6.89 (d, 1H, *J* = 8.4 Hz), 6.65 (dd, 1H, *J* = 8.7, 1.6 Hz), 6.49 (s, 1H), 6.46 (d, 1H, *J* = 2.7 Hz), 5.61 (d, 1H, *J* = 9.8 Hz), 5.09 (d, 1H, *J* = 6.5 Hz), 4.83 (m, 1H), 3.82 (s, 3H), 3.76 (s, 3H), 3.74 (s, 3H), 3.06 (d, 1H, *J* = 5.6 Hz), 3.00 (s, 1H), 1.39 (s, 3H). 1.37 (s, 1H); HRMS (FAB) calcd for $C_{22}H_{25}FO_6$ (M^+): 404.1635. Found: 404.1635.

3.42. (*rel*-1S,2S)-1-(5,6-Dimethoxypyridin-2-yl)-2-(5-methoxy-2,2-dimethyl-2H-chromen-6-yl)ethane-1,2-diol (49).

Compound **49** was synthesized from compound **47** through diolation following procedure J, 45% yield, brown solid, mp = 79-80 ^{o}C; ^{1}H-NMR ($CDCl_3$, 300MHz) δ 7.17 (d, 1H, *J* = 8.4 Hz), 6.93 (d, 1H, *J* = 8.1 Hz), 6.60 (m, 2H), 6.50 (dd, 1H, *J* = 9.9, 0.6 Hz), 5.65 (d, 1H, *J* = 9.9 Hz), 5.00 (m, 1H), 4.78 (m, 1H), 4.01 (s, 3H), 3.84 (s, 3H), 3.65 (s, 3H), 1.43 (s, 3H), 1.40 (s, 3H); HRMS (FAB) calcd for $C_{21}H_{26}NO_6$ ($M + H^+$): 388.1760. Found: 388.1755.

3.43. (*E*)-2-(5,6-Dimethoxypyridin-2-yl)-1-(5-methoxy-2,2-dimethyl-2H-chromen-6-yl)ethan-1-one oxime (50a).

Compound **50a** was synthesized from compound **12** through oximation following procedure K, 40% yield, yellow solid, mp = 69-70 ^{o}C; ^{1}H-NMR ($CDCl_3$, 300MHz) δ 7.00 (d, 1H, *J* = 8.4 Hz), 6.92 (d, 1H, *J* = 7.9 Hz), 6.74 (d, 1H, *J* = 9.9 Hz), 6.58 (d, 1H, *J* = 9.9 Hz), 6.50 (d, 1H, *J* = 8.4 Hz), 5.63 (d, 1H, *J* = 10.1 Hz), 4.19 (s, 2H), 3.89 (s, 3H), 3.81 (s, 3H), 3.66 (s, 3H), 1.41 (s, 6H); HRMS (FAB) calcd for $C_{21}H_{25}N_2O_5$ ($M + H^+$): 385.1763. Found: 385.1759.

3.44. (*Z*)-2-(5,6-Dimethoxypyridin-2-yl)-1-(5-methoxy-2,2-dimethyl-2H-chromen-6-yl)ethan-1-one oxime (50b).

Compound **50b** was synthesized from compound **12** through oximation following procedure K, 25% yield, yellow solid, mp = 68-69 ^{o}C; ^{1}H-NMR ($CDCl_3$, 300MHz) δ 6.90 (d, 1H, *J* = 7.9 Hz), 6.76 (d, 1H, *J* = 8.4 Hz), 6.67 (d, 1H, *J* = 7.9 Hz), 6.58 (d, 1H, *J* = 10.1 Hz), 6.48 (d, 1H, *J* = 8.4

Hz), 5.61 (d, 1H, *J* = 9.9 Hz), 3.89 (s, 3H), 3.87 (s, 2H), 3.80 (s, 3H), 3.72 (s, 3H), 1.42 (s, 6H); HRMS (FAB) calcd for $C_{21}H_{25}N_2O_5$ ($M + H^+$): 385.1763. Found: 385.1769.

3.45. (*Z*)-2-(5,6-Dimethoxypyridin-2-yl)-1-(5-methoxy-2,2-dimethyl-2H-chromen-6-yl)ethan-1-one O-methyl oxime (51).

Compound **51** was synthesized from compound **12** through oximation following procedure K, 38% yield, pale yellow oil; ^{1}H-NMR ($CDCl_3$, 400MHz) δ 7.02 (d, 1H, *J* = 8.4 Hz), 6.87 (d, 1H, *J* = 7.9 Hz), 6.65 (d, 1H, *J* = 7.8 Hz), 6.54 (d, 1H, *J* = 10.0 Hz), 6.47 (d, 1H, *J* = 8.2 Hz), 5.60 (d, 1H, *J* = 9.9 Hz), 4.12 (s, 2H), 3.94 (s, 3H), 3.82 (s, 2H), 3.78 (s, 3H), 3.71 (s, 3H), 1.36 (s, 6H); HRMS (FAB) calcd for $C_{22}H_{27}N_2O_5$ ($M + H^+$): 399.1920. Found: 399.1915.

3.46. 2-(5,6-Dimethoxypyridin-2-yl)acetic acid (52).

To a solution of compound **6** in DCM was added $SOCl_2$ (1.5 equiv) dropwise at 0 ^{o}C. After being stirred for 30 min, the mixture was evaporated to remove excess amount of $SOCl_2$ and directly used for the next step. The chlorinated compound was dissolved in DMSO. Sodium cyanide (1.5 equiv) was slowly added to the solution at 0 ^{o}C. The mixture was warmed to 60^{o}C and stirred for 2 h. The resulting solution was cooled down to room temperature, extracted with DCM, dried over $MgSO_4$, and concentrated under reduced pressure. The residue was purified by flash column chromatography on silica gel to afford the corresponding nitrile product 80% yield. The nitrile compound was dissolved in the solvent (EtOH : H_2O = 1:1). Potassium hydroxide (5.0 equiv) was added to the solution and stirred 2 h. The reaction mixture was cooled to 0 ^{o}C, neutralized with 1N HCl, extracted with MC. Organic layer was dried over $MgSO_4$, and concentrated under reduced pressure to afford the corresponding carboxylic acid product **52**, 86% yield; ^{1}H-NMR ($CDCl_3$, 300MHz) δ 7.11 (d, 1H, *J* = 7.9 Hz), 6.79 (d, 1H, *J* = 8.0 Hz), 4.05 (s, 3H), 3.88 (s, 3H), 3.75 (s, 2H)

3.47. (*S*)-4-Benzyl-3-((*S*)-2-(5,6-dimethoxypyridin-2-yl)propanoyl)oxazolidin-2-one (53).

(*S*)-4-benzyloxazolidin-2-one (1.0 equiv) was dissolved in THF. 2.5 M n-BuLi solution in hexane (1.0 equiv) was added to the solution at -78 ^{o}C. On another flask, in a solution of carboxylic acid **52** in anhydrous THF, pivaloylchloride (1.1 equiv) and TEA (1.1 equiv) was added dropwise at -78^{o}C. The reaction mixture was warmed to 0 ^{o}C. This mixture was added to the former solution at -78 ^{o}C. The final mixture was stirred for 1 h, quenched wih water, extracted with EtOAc, dried over $MgSO_4$

and concentrated. The residue was purified by flash column chromatography on silica gel to afford oxazolidinone compound, 60% yield.

This compound was dissolved in anhydrous THF. 1.0 M LiHMDS solution (1.0 equiv) was added to the solution at -78 ^{o}C. The mixture was stirred for 20 min and iodomethane (1.0 equiv) was added to this solution. The resulting solution was stirred for another 30 min, quenched with water, extracted with EtOAc, dried over $MgSO_4$ and concentrated. The residue was purified by flash column chromatography on silica gel to afford (*S*)-mono methylated compound **53**, 40% yield; ^{1}H-NMR ($CDCl_3$, 400MHz) δ 7.36-7.22 (m, 5H), 7.00 (d, 1H, *J* = 7.9 Hz), 6.87 (d, 1H, *J* = 7.9 Hz), 5.09 (q, 1H, *J* = 7.0 Hz), 4.65 (m, 1H), 4.13 (m, 2H), 3.96 (s, 3H), 3.92 (s, 3H), 3.37 (dd, 1H, *J* = 13.2, 3.1 Hz), 2.81 (dd, 1H, *J* = 13.2, 3.1 Hz), 1.56 (d, 3H, *J* = 7.0 Hz).

3.48. (*S*)-2-(5,6-Dimethoxypyridin-2-yl)propanal (54).

To a solution of compound **53** in anhydrous Et_2O, LAH (1.0 equiv) was added slowly at 0 ^{o}C. The reaction mixture was stirred for 1 h, quenched with water and 1 N NaOH solution. The organic layer was extracted with EtOAc, dried over $MgSO_4$ and concentrated. The residue was purified by flash column chromatography on silica gel to afford alcohol compound, 90% yield. This alcohol compound was dissolved in MC and oxidized following the procedure B to afford aldehyde compound **54**, 90% yield; ^{1}H-NMR ($CDCl_3$, 300MHz) δ 9.79 (s, 1H), 7.03 (d, 1H, *J* = 7.9 Hz), 6.74 (d, 1H, *J* = 7.7 Hz), 4.00 (s, 3H), 3.88 (s, 3H), 3.63 (q, 1H, *J* = 7.1 Hz), 1.44 (d, 3H, *J* = 7.1 Hz)

3.49. 6-Iodo-5-methoxy-2,2-dimethyl-2H-chromene (56).

To a solution of compound **55** (1.0 mmol) in H_2O, KI (2.0 mmmol) was mixed and then 1 drop of c-HCl was added at 0 ^{o}C. $NaNO_2$ was slowly added to the mixture at 0 ^{o}C. The resulting solution was stirred for 30 min. Then the mixture was extracted with EA, washed with brine, water and the organic phase was dried over $MgSO_4$ and concentrated. The residue was purified by flash column chromatography on silica gel to afford iodo compound **56**, 90% yield; ^{1}H-NMR ($CDCl_3$, 300MHz) δ 7.45 (d, 1H, *J* = 8.6 Hz), 6.55 (d, 1H, *J* = 10.1 Hz), 6.39 (d, 1H, *J* = 8.6 Hz), 5.64 (d, 1H, *J* = 10.1 Hz), 3.82 (s, 3H), 1.87 (s, 6H)

3.50. (*S*)-2-(5,6-Dimethoxypyridin-2-yl)-1-(5-methoxy-2,2-dimethyl-2H-chromen-6-yl)propan-1-one (16*S*).

Chrial compound **16*S*** was synthesized from iodo compound **56** and aldehyde **54** through procedure A followed by procedure B, 35% yield, pale yellow oil; $[\alpha]^{25}_{D}$ -79.6(*c* 0.1, $CHCl_3$), ^{1}H-NMR ($CDCl_3$, 300MHz) δ 7.46 (d, 1H, *J* = 8.6 Hz), 6.94 (d, 1H, *J* = 7.9 Hz), 6.77 (d, 1H, *J* = 7.9 Hz), 6.58 (d, 1H, *J* = 10.1 Hz), 6.52 (dd, 1H, *J* = 8.4, 0.6 Hz), 5.64 (d, 1H, *J* = 10.1 Hz), 4.74 (q, 1H, *J* = 7.0 Hz), 3.91 (s, 3H), 3.81 (s, 3H), 3.75 (s, 3H), 1.51 (d, 1H, *J* = 7.0 Hz), 1.42 (s, 3H), 1.41(s, 3H); HRMS (FAB) calcd for $C_{22}H_{26}NO_5$ ($M + H^+$): 384.1811. Found: 384.1808.

4. Molecular modeling

All performances of computational works were carried out on the Tripos Sybyl-X 2.1[1] molecular modeling package with CentOS Linux 5.4. operating system.

4.1. Preparation of ligands and prepare structure

All used ligands for docking screening were sketched and saved as Mol2 format. Gasteiger-Hückel charges were assigned to all ligand atoms. Energy minimization was performed with the standard tripos force field with convergence to maximum derivatives of 0.001 kcal $mol^{-1}.Å^{-1}$. It was reported that the function of HSP90 C-terminal inhibitors was related with binding to the open form of homodimer HSP90 structure.[30] Therefore, we built the homology model of open conformation of human Hsp90 dimer based on the extended SAXS model of *E. coli* HSP90 homodimer including N-, middle and C-terminal domain. Homology modeling was performed with ORCHESTRAR[3] module. The template structure was retrieved from Agard' lab website (http://www.msg.ucsf.edu/agard, PDB id: hsp90). The sequence identity of Hsp90 between E-coli and human is 42.9%. In the first step, alignment file was defined using complete partial model. Next, based on this alignment file, structurally conserved regions (SCRs) were built automatically and variable region was also identified. Loops were optimized by loop-search option and side chains were modified with set side chain option. The resulting homology model structure was optimized by minimization with assigning Kollman all charges to all the atoms of protein and convergence to maximum derivatives of 0.05 kcal $mol^{-1}.Å^{-1}$.

4.2. Molecular docking

To exam docking pose of **25**, the compound was docked into the active site of *h*HSP90 using Surflex-Dock embedded in Sybyl. The active site was determined based on the ATP binding pocket the C-terminal domain[2] and was generated by constructing protomol.The protomol was built in the active site from the hydrogen-containing protein mol2 file using default parameters (threshold factor of 0.5Å and bloat of 0Å). Docking was conducted using default parameters such as 6

additional starting conformations per molecule and 6 Å to expand search grid. Max number of conformations per fragment was 20, and 100 max number of rotatable bond was used for parameters and flags. For output, 20 maximum number of poses per ligand were generated. Binding affinity of each docking pose of ligand was calculated by Surflex-Dock score (-log K_d). The final docking model was selected by docking score and visual inspection.